TECHNICAL DOCUMENTATION

1976?

2, 3, & 4 AXLE RIGID TRUCK CURVE NEGOTIATION MODEL

K. R. Smith
R. D. MacMillan
G. C. Martin

MATHEMATICAL MODEL

MATHEMATICAL MODEL

national Government-Industry
...ch Program on Track-Train Dynamics

R-206

TECHNICAL DOCUMENTATION

2, 3, & 4 AXLE RIGID TRUCK CURVE NEGOTIATION MODEL

K. R. Smith
R. D. MacMillan
G. C. Martin

MATHEMATICAL MODEL

MATHEMATICAL MODEL

An International Government-Industry Research Program on Track-Train Dynamics

Steering Committee for the Track Train Dynamics Program

Chairman
J. L. Cann
Vice President
Operation and Maintenance
Canadian National Railways

Vice Chairman
W. J. Harris, Jr.
Vice President
Research and Test Department
Association of American Railroads

E. F. Lind
Project Director-Phase I
Track Train Dynamics
Southern Pacific Transportation Co.

M. D. Armstrong
Chairman
Transportation Development Agency
Canadian Ministry of Transport

W. S. Autrey
Chief Engineer
Atchison, Topeka & Santa Fe Railway Co.

M. W. Bellis
Manager
Locomotive Engineering
General Electric Company

M. Ephraim
Chief Engineer
Electro Motive Division
General Motors Corporation

J. G. German
Vice President
Engineering
Missouri Pacific Co.

W. S. Hansen
President
A. Stucki Co.

W. P. Manos
Vice President
Research and Development
Pullman-Standard

R. A. Matthews
Vice President
Railway Progress Institute

R. G. Maughan
Chairman
Railroad Advisory Committee
Transportation Development Agency

D. K. McNear
Vice President
Operations
Southern Pacific Transportation Co.

L. A. Peterson
Director
Office of Rail Safety Research
Federal Railroad Administration

G. E. Reed
Director
Railroad Sales
AMCAR Division
ACF Industries

D. V. Sartore
Chief Engineer Design
Burlington Northern, Inc.

P. S. Settle
President
Railway Maintenance Corporation

W. W. Simpson
Vice President
Engineering
Southern Railway System

W. S. Smith
Vice President and
Director of Transportation
General Mills, Inc.

J. B. Stauffer
Director
Transportation Test Center
Federal Railroad Administration

*R. D. Spence (Chairman)
President
ConRail

*L. S. Crane (Chairman)
President and Chief
Administrative Officer
Southern Railway System

*D. Y. Clem (Vice Chairman)
President
McConway & Torley Corporation

*C. Bruce Ward (Vice Chairman)
President
Gunderson, Inc.

*Edward J. Ward (Vice Chairman)
Acting Associate Administrator for
Research and Development
Federal Railroad Administration

*Former members of this committee

BACKGROUND INFORMATION

on the

TRACK-TRAIN DYNAMICS PROGRAM

The Track-Train Dynamics Program encompasses studies of the dynamic interaction of a train consist with track as affected by operating practices, terrain, and climatic conditions.

Trains cannot move without these dynamic interactions. Such interactions, however, frequently manifest themselves in ways climaxing in undesirable and costly results. While often differing and sometimes necessarily so, previous efforts to reasonably control these dynamic interactions have been reflected in the operating practices of each railroad and in the design and maintenance specifications for track and equipment.

Although the matter of track-train dynamics is by no means a new phenomena, the increase in train lengths, car sizes and loadings has emphasized the need to reduce wherever possible excessive dynamic train action. This, in turn, requires a greater effort to achieve more control over the stability of the train as speeds have increased and railroad operations become more systematized.

The Track-Train Dynamics Program is representative of many new programs in which the railroad industry is pooling its resources for joint study and action.

A major planning effort on track-train dynamics was initiated in July 1971 by the Southern Pacific Transportation Company under contract to the AAR and carried out with AAR staff support. Completed in early 1972, this plan clearly indicated that no individual railroad has both the resources and the incentive to undertake the entire program. Therefore, AAR was authorized by its Board to proceed with the Track-Train Dynamics Program.

In the same general period, the FRA signaled its interest in vehicle dynamics by development of plans for a major test facility. The design of a track loop for train dynamic testing and the support of related research programs were also pursued by FRA.

In organizing the effort, it was recognized that a substantial body of information and competence on this program resided in the railroad supply industry and that significant technical and financial resources were available in government.

Through the Railway Progress Institute, the supply industry coordinated its support for this program and has made available men, equipment, data from earlier proprietary studies, and monetary contributions.

Through the FRA, contractor personnel and direct financial resources have been made available.

Through the Transportation Development Agency, the Canadian Government has made a major commitment to work on this problem and to coordinate that work with the United States' effort.

Through the Office de Recherches et D'Essais, the research arm of the Union Internationale des Chemins de Fer, the basis for a full exchange of information with European groups active in this field has been arranged.

The Track-Train Dynamics Program is managed by the Research and Test Department of the Association of American Railroads under the direction of an industry-government steering committee. Railroad members are designated by elected members of the AAR's Operation-Transportation General Committee, supply industry members by the Railway Progress Institute, U.S. Government members by the Federal Railroad Administration, and Canadian Government members by the Transportation Development Agency. Appropriate task forces and advisory groups are established by the steering committee on an ad hoc basis, as necessary to pursue and resolve elements of the program.

The staff of the program comprises AAR employees, personnel contributed on a full- or part-time basis by railroads or members of the supply industry, and personnel under contract to the Federal Railroad Administration or the Transportation Development Agency.

The program plan as presented in 1972 comprised:

1) Phase I -- 1972-1974

   Analysis of and interim action regarding the present dynamic aspects of track, equipment, and operations to reduce excessive train action.

2) Phase II -- 1974-1977

   Development of improved track and equipment specifications and operating practices to increase dynamic stability.

3) Phase III - 1977-1982

   Application of more advanced scientific principles to railroad track, equipment, and operations to improve dynamic stability.

Phase I officially ended in December of 1974. The major technical elements of Phase I included:

a) The establishment of the dynamic characteristics of track and equipment.

b) The development and validation of mathematical models to permit the rapid analysis of the effects on dynamic stability of modifications in design, maintenance, and use of equipment and track structures.

c) The development of interim guidelines for train handling, makeup, track structures, and engineer training to reduce excessive train action.

The attached report presents the Technical Manual Documentation for the 2, 3, and 4 Axle Rigid Truck Curve Negotiation Model, which was developed as an element of item b) above.

ACKNOWLEDGEMENT

The contents of this manual are largely based upon a program developed by Mr. Karl R. Smith of Electro Motive Division, General Motors Corporation. Further development and enhancements have been made by Mr. R. MacMillan, Research Engineer, and Dr. G. C. Martin, Deputy Project Director of Track-Train Dynamics, and Director - Dynamics Research, of the AAR Research and Test Department.

Also, the authors wish to acknowledge Mr. Edward F. Lind, Project Director, Phase I of the Track-Train Dynamics Research Program. Mr. Lind's leadership has been a major contributing factor to the entire success of the Track-Train Dynamics Research Program--a program which has and will continue to produce significant contributions to the railroad industry for years to come.

Finally, the contribution by Electro Motive Division, General Motors Corporation in the model development is deeply appreciated.

This program was developed as part of an effort in Task #7, Mathematical Modelling, of Phase I of the Track-Train Dynamics Research Program.

TABLE OF CONTENTS

TABLE OF CONTENTS (Continued)

1. INTRODUCTION

The interaction between the wheels of a locomotive truck and the rail have long been of great interest to design and operating personnel associated with railroads, and much in the way of theoretical and field test work has been done to learn more of the subject referred to as "Curve Negotiation Mechanics". It has been learned that the single most important key to understanding curve negotiation is to be able to identify and solve for the phenomenon of friction and creep occurring at the wheel-rail interface. Once this has been accomplished, the flange reactions or curving forces may be determined.

An understanding of curve negotiation mechanics is vital from the standpoint of learning of the design and operating parameters that result in decreases and increases in the lateral reaction occurring between the wheel flange and rail, for it is this lateral load that results in wear on the wheel and rail, determines if a wheel will climb the rail during curving or if the entire track structure will shift. Aside from the more obvious considerations of tracking, lies the importance of an understanding of curving from the design standpoint. It must be known how much clearance should exist in a rigid framed truck to allow negotiation of sharp curves and what loads may be expected, so that proper design for strength can be accomplished.

The objective, then, of this study is to develop a technique by which the wheel/rail interaction associated with the negotiation of a section of curved track by a rigid framed

locomotive truck may be predicted for various arbitrary operating conditions, such as:

- Any combinations of individual axle loads.
- Any combinations of individual wheel loads.
- Operation at over or under balance speed.
- Development of a tractive or braking effort.
- Train operation forces which may result in buff or drag force components at the truck center bearing.

Section 2 discusses the friction-creep phenomenon and its solution, while Section 3 gives an explanation of the various possible curving constraint modes. In Section 4, the external loads to be considered are outlined, and Section 5 discusses the physical model to which they will be applied. Sections 6 and 7 describe the method of solution and the results of that solution, respectively.

2. CURVING FORCES

The term "Curve Negotiation Forces" is used to describe the lateral and longitudinal forces (with respect to the track) that result from the traversing of a portion of curved track by a rigid locomotive truck. The curve negotiation forces may be broken down into two (2) general categories:

1. Friction-Creep Forces
2. Wheel Flange Forces

In terms of cause and effect terminology, the friction-creep forces would be considered the cause as they are the direct result of steady state curving with no forces applied externally (lateral center plate loads, etc.) to the truck. The wheel flange forces would then be considered to be the effect, or those reactions necessary to maintain the truck in a force equilibrium balance. When externally applied forces are present they will be balanced by either wheel flange forces, friction-creep forces, or combinations thereof.

2.1 Friction-Creep Relationships & Forces

Consider a wheel/axle set in which both wheels are rigidly mounted on the axle. As this assembly rolls around a curved segment of track, the distance that must be traversed by the outer wheel is greater than that distance which must be traversed by the inner wheel. The taper on the wheel will compensate for only a small amount of this distance in rolling distance and since both wheels are assumed to be rigidly mounted on the axle, the remaining

portion must be dissipated as a relative slip between the rail and wheels. The slip may be more specifically thought of as a slip velocity, as that is what in actuality it is, a difference in the rolling velocity of the wheel and the relative rail velocity at their contact point. This slip, when coupled with the normal load acting on the wheel, gives rise to a frictional force which acts in the same direction as the slip velocity. Due to the fact that the wheel/axle set is considered to be a rigid body, the longitudinal components of the frictional force acting at each wheel will impart a couple which will rotate the assembly about a vertical axis. The couple imparted to the wheel/axle assembly will be transmitted into the truck frame where it combines with additional couples generated in a similar fashion at other axles. With this assumption of a rigid frame truck such that the axles are constrained to remain parallel to one another at all times, there will be a common instantaneous center of rotation for the truck frame and each axle. This instantaneous center of rotation may also be referred to as the "friction center", as the slip velocity, hence friction force, at each wheel will act perpendicularly to a line drawn between the wheel/rail contact point and the friction center.

2.2 Slip Velocities

In this analysis of slip, the effect of wheel coning is not taken into account as its effect on the longitudinal creep is assumed to be very small in comparison to the lon-

gitudinal slip developed from the difference in rolling distance of each wheel of the wheel/axle set.

Consider a rigid wheel/axle set as it traverses a segment of curved track at some arbitrary velocity. Figure 1 shows a wheelset of a rigid truck with its friction center (instantaneous center of rotation) at a perpendicular distance D1 from the axle. The assembly is shown with the friction center displaced an arbitrary distance S radially outward from the truck centerline which in turn makes a small yaw or misalignment angle α with the rail. The curve is of constant radius R, and the radius vectors from the friction center and wheel/rail contact point to the center of curvature make angles ϕ and θ, respectively, with a fixed X-Y rectangular coordinate system parallel to the truck centerline.

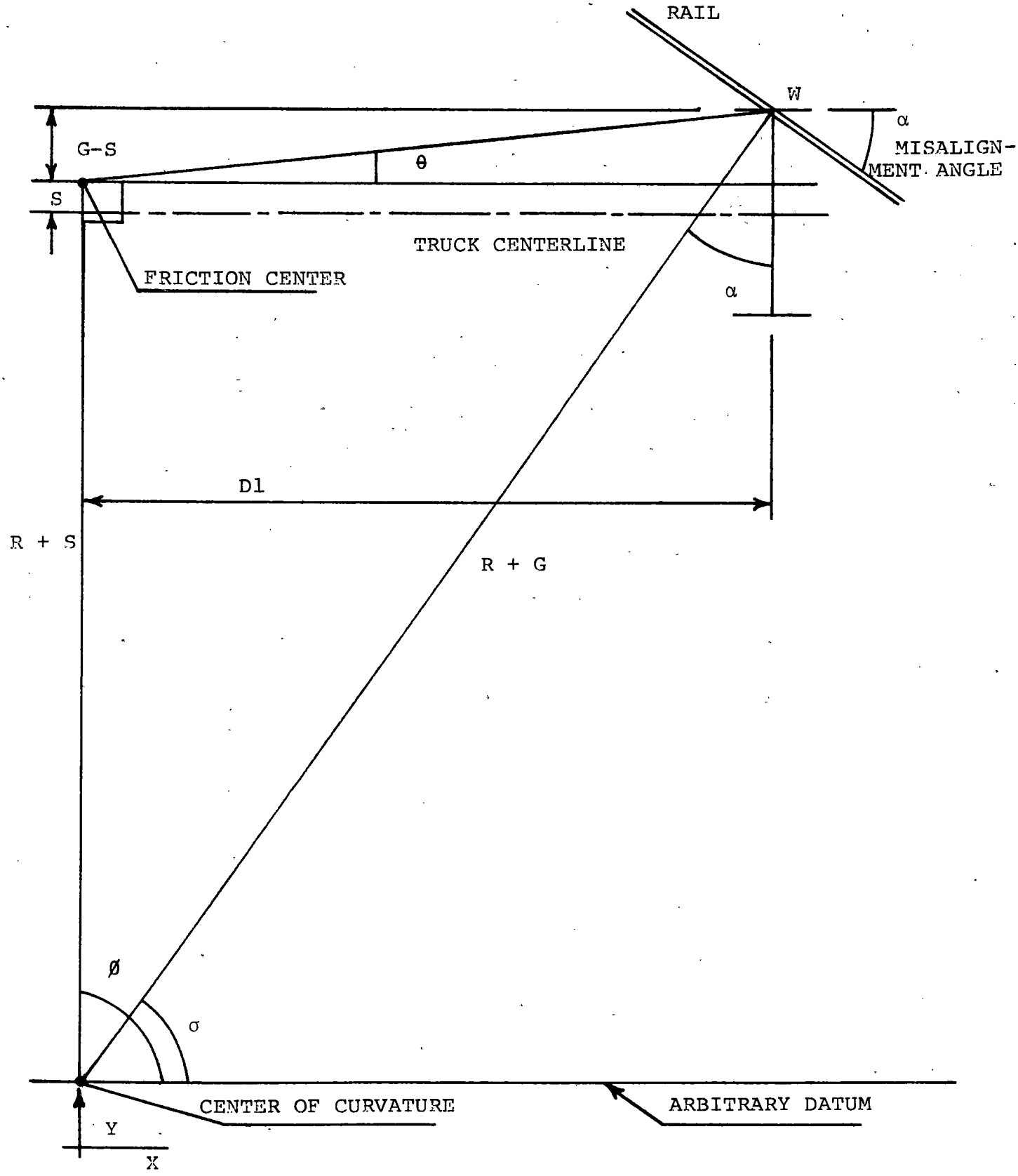
RAIL
W
α
MISALIGN-
MENT ANGLE
G-S
θ
S
TRUCK CENTERLINE
FRICTION CENTER
α
D1
R + S
R + G
ø
σ
CENTER OF CURVATURE
ARBITRARY DATUM
Y
X

FIGURE 1

At any instant of time the contact point on the wheel with the rail, W, may be located with respect to the center of curvature, C, in the X and Y directions as:

$$W_X = (R+S)\ \cos\phi + (D1^2 + (G-S)^2)^{\frac{1}{2}}\ \cos\theta \qquad (1)$$

$$W_Y = (R+S)\ \sin\phi + (D1^2 + (G-S)^2)^{\frac{1}{2}}\ \sin\theta \qquad (2)$$

The wheel/rail contact point on the rail, WR, may be located at the same instant in both the X and Y direction as:

$$WR_X = (R+G)\ \cos\sigma \qquad (3)$$

$$WR_Y = (R+G)\ \sin\sigma \qquad (4)$$

The velocities of the wheel W, and rail WR, contact points may be found by differentiation of equations (1) thru (4) with respect to time.

$$\frac{dW_x}{dt} = V_{wx} = -(R+S)\sin\phi\ \dot{\phi} - (D1^2+(G-S)^2)^{\frac{1}{2}}\ \sin\theta\ \dot{\theta} \qquad (5)$$

$$\frac{dW_y}{dt} = V_{wy} = (R+G)\cos\phi\ \dot{\phi} + (D1^2+(G-S)^2)^{\frac{1}{2}}\ \cos\theta\ \dot{\theta} \qquad (6)$$

$$\frac{dWRx}{dt} = V_{wrx} = -(R+G)\sin\sigma\ \dot{\sigma} \qquad (7)$$

$$\frac{dWRy}{dt} = V_{wry} = (R+G)\cos\sigma\ \dot{\sigma} \qquad (8)$$

With the wheelset negotiating the curve at some steady state velocity V the friction center must also translate at the same velocity, or with respect to the center of curvature:

$$V = (R+S)\,\dot{\phi} \tag{9}$$

It can also be seen that for the system where D1 remains constant for steady state curving:

$$\dot{\sigma} = \dot{\phi} \tag{10}$$

The slip velocities between the wheel and rail may be computed as the difference in the X and Y components of the rail and wheel velocities. Recalling equations (6) and (8), the lateral slip velocity (Y-direction) will be:

$$S_{LAT} = V_{wry} - V_{wy}$$

$$S_{LAT} = \dot{\sigma}(R+G)\,\cos\sigma - \dot{\phi}(R+S)\,\cos\phi - \dot{\theta}\,(D1^2 + (G-S)^2)^{\frac{1}{2}}\,\cos\theta \tag{11}$$

Substituting equation (10):

$$S_{LAT} = \dot{\phi}\,\left[(R+G)\,\cos\sigma - (R+S)\,\cos\phi\right] - \dot{\theta}\,(D1^2 + (G-S)^2)^{\frac{1}{2}}\,\cos\theta \tag{12}$$

From geometry in Figure 1, COS θ may be obtained as:

$$\cos\theta = D1/(D1^2 + (G-S)^2)^{\frac{1}{2}} \tag{13}$$

Substitution of equation (13) into equation (12) yields the lateral slip velocity equation:

$$S_{LAT} = \dot{\phi}\,\left[(R+G)\,\cos\sigma - (R+S)\,\cos\phi\right] - D1\,\dot{\theta} \tag{14}$$

In a similar manner the longitudinal slip velocity (X-direction) may be found as the difference between the longitudinal velocity components of the rail and wheel.

Recalling equations (5) and (7):

$$S_{LONG} = V_{wrx} - V_{wx}$$

$$S_{LONG} = -\dot{\sigma}(R+G)\ SIN\sigma + \dot{\phi}\ (R+S)\ SIN\ \phi + \dot{\theta}\ (Dl^2 + (G-S)^2)^{\frac{1}{2}}\ SIN\ \theta \quad (15)$$

$$S_{LONG} = \dot{\phi}\ [(R+S)\ SIN\ \phi - (R+G)\ SIN\sigma] + \dot{\theta}\ (Dl^2 + (G-S)^2)^{\frac{1}{2}} SIN\ \theta \quad (16)$$

From Figure 1, SIN θ may be obtained as:

$$SIN\ \theta = (G-S)/(Dl^2 + (G-S)^2)^{\frac{1}{2}} \quad (17)$$

Substitution of equation (17) into equation (16) yields the longitudinal slip velocity equation:

$$S_{LONG} = \dot{\phi}\ [(R+S)\ SIN\ \phi - (R+G)\ SIN\sigma] + (G-S)\ \dot{\theta} \quad (18)$$

Once the geometrical relationships for SIN ϕ, SIN σ, COS ϕ, and COSσ have been computed, the actual slip magnitudes may be determined. Refer to Appendix "A" for the computation of the SIN, COS terms which are found to be:

$$COS\ \sigma = Dl/(R+G)$$

$$SIN\ \sigma \simeq 1.0$$

$$COS\ \phi \simeq 0.0$$

$$SIN\ \phi \simeq 1.0$$

The lateral slip velocity (14) may now be rewritten as:

$$S_{LAT} = \dot{\phi}\ \left[(R+G)\ \frac{Dl}{R+G} - (R+S) \cdot 0\right] - Dl\ \dot{\theta} \quad (19)$$

$$S_{LAT} = Dl\ (\dot{\phi} - \dot{\theta}) \quad (20)$$

For steady state curving at a constant radius, it may be seen that θ must be equal to zero, hence:

$$S_{LAT} = Dl\ \dot{\phi} \quad (21)$$

The lateral slip velocity component may now be written in terms of velocity terms by inserting equation (9) into (21):

$$S_{LAT} = \frac{V \cdot D1}{(R+S)} \tag{22}$$

The longitudinal slip velocity (18) will become:

$$S_{LONG} = \dot{\phi}\left[(R+S) - (R+G)\right] + (G-S)\,\dot{\theta} \tag{23}$$

Making the substitutions for $\dot{\phi}$ and $\dot{\theta}$:

$$S_{LONG} = \frac{V\,(S-G)}{(R+S)} \tag{24}$$

2.3 Resultant Creep

The friction forces that arise from curve negotiation are a function of the total slip or displacement that occurs between the wheel and rail at their contact points. This relative displacement is commonly called creep and may be defined as the slip velocity divided by the roll velocity, where the roll velocity is the actual velocity of the wheelset, or in a more specific sense, of the friction center. Therefore, the lateral creep may be written as:

$$CREEP_{LAT} = S_{LAT}/V \tag{25}$$

Inserting the lateral slip velocity term (22) into (25) gives the term for the magnitude of lateral creep component:

$$CREEP_{LAT} = D1/(R+S) \tag{26}$$

Similarly, the magnitude of the longitudinal creep components may be found as:

$$CREEP_{LONG} = (S-G)/(R+S) \tag{27}$$

It is known that the friction-creep curves for longitudinal and lateral creep differ from one another, both in slope and the peak coefficient of friction attainable. It is, therefore, helpful to define a resultant creep in cases where theoretical or experimental friction-creep relationships have been established as a function of a net or resultant creep. This is beneficial from the standpoint that the direction of the resultant creep at a wheel will be normal to a line extending through the wheel-rail contact point and friction center. This may be more readily visualized when recalling that the resultant slip velocity at each wheel acts in the same direction as the resultant creep of friction force, and due to the rigid body assumption that velocity at any point must act perpendicularly to a line drawn through that point and the instantaneous center of rotation (friction center).

The resultant creep may now be determined by combining the lateral and longitudinal creep components at the wheel to get: +

$$\text{RESULTANT CREEP} = A = (D1^2 + (S-G)^2)^{\frac{1}{2}} / (R+S)$$

Thus far we have been investigating only a wheel on the outer* rail so that the resultant creep derived is for

* Note: The term outer wheel is used to describe a a wheel whose contact point with the rail is at a greater distance from the center of curvature than the friction centers distance to the center of curvature, and vice versa for an inner wheel.

\+ See "Appendix C" for modification to this equation due to radius differential creep.

any wheel on the outer or high rail side of the curve, therefore:

$$A = A_o = (Dl^2 + (S-G)^2)^{\frac{1}{2}} / (R+S) \quad (28)$$

It can be shown in a similar fashion (see Appendix "B") that the resultant creep on the inner or low rail side of the curve will be:+

$$A_i = (Dl^2 + (S+G)^2)^{\frac{1}{2}} / (R+S) \quad (29)$$

With the resultant creep known at each wheel the coefficient of friction may be found from the friction creep curve (similar to that shown in Figure 16), and combined with the vertical wheel load to give the frictional force acting at each wheel. These forces may then be added to the truck wheelsets as depicted by Figure 2.

The appearance of the S term in the creep equations indicates that both wheels on the same axle must not necessarily develop equal creeps, but that they may vary in both magnitude and direction. This type of occurrence is most commonly found when the vertical wheel loads differ from one side to the other or a tractive effort, braking effort, or buff condition is present.
The friction-creep force orientation depicted in Figure 2 is typical for coasting through a curve with little or no lateral center plate load, tractive or braking effort, or buff force present. Here it can be seen that the outer wheels have a tendency to creep rearwards, while the inner wheels creep forwards.

+ See "Appendix C" for modification of this equation due to radius differential creep.

TYPICAL FRICTION FORCE LOCATION AND SENSE FOR A THREE-AXLE TRUCK

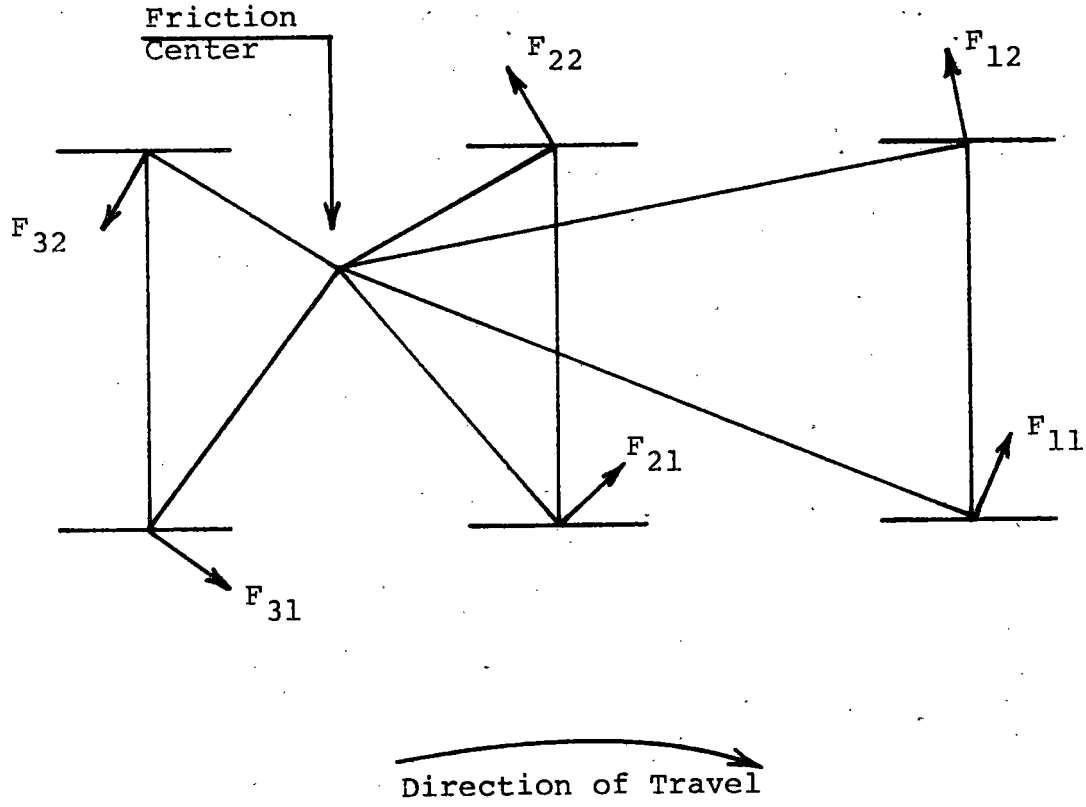

FIGURE 2

3. CURVING MODES

There are a number of different configurations that a rigid framed truck may be in as it traverses a curved portion of track, all of which may be characterized by the relationship of the wheels with respect to the rails. These various modes of curving are more commonly referred to as degrees of constraint and are diagrammed in Figure 3.

3.1 Free Curving

The term free curving is used to describe that realm of curve negotiation where the leading outer wheel is in flange contact with the outer rail, and the trailing inner wheel is disposed toward the inner rail; however, there is no flange contact. For a 3 or 4-axle truck the second outer wheel may or may not be in flange contact with the outer rail. This is dependent on the axle lateral suspension, friction force present and the axle to truck frame free clearance designed into the truck, as when the friction center is behind the second axle the resultant friction force is such that the axle will be disposed outward.

3.2 First Degree Constraint

First degree constraint is used to describe the curving mode that is typified by the leading outer wheel being in flange contact with the outer rail, and the trailing inner wheel in flange contact with the inner

MODES OF CURVING

2, 3, & 4-Axle Rigid Framed Trucks

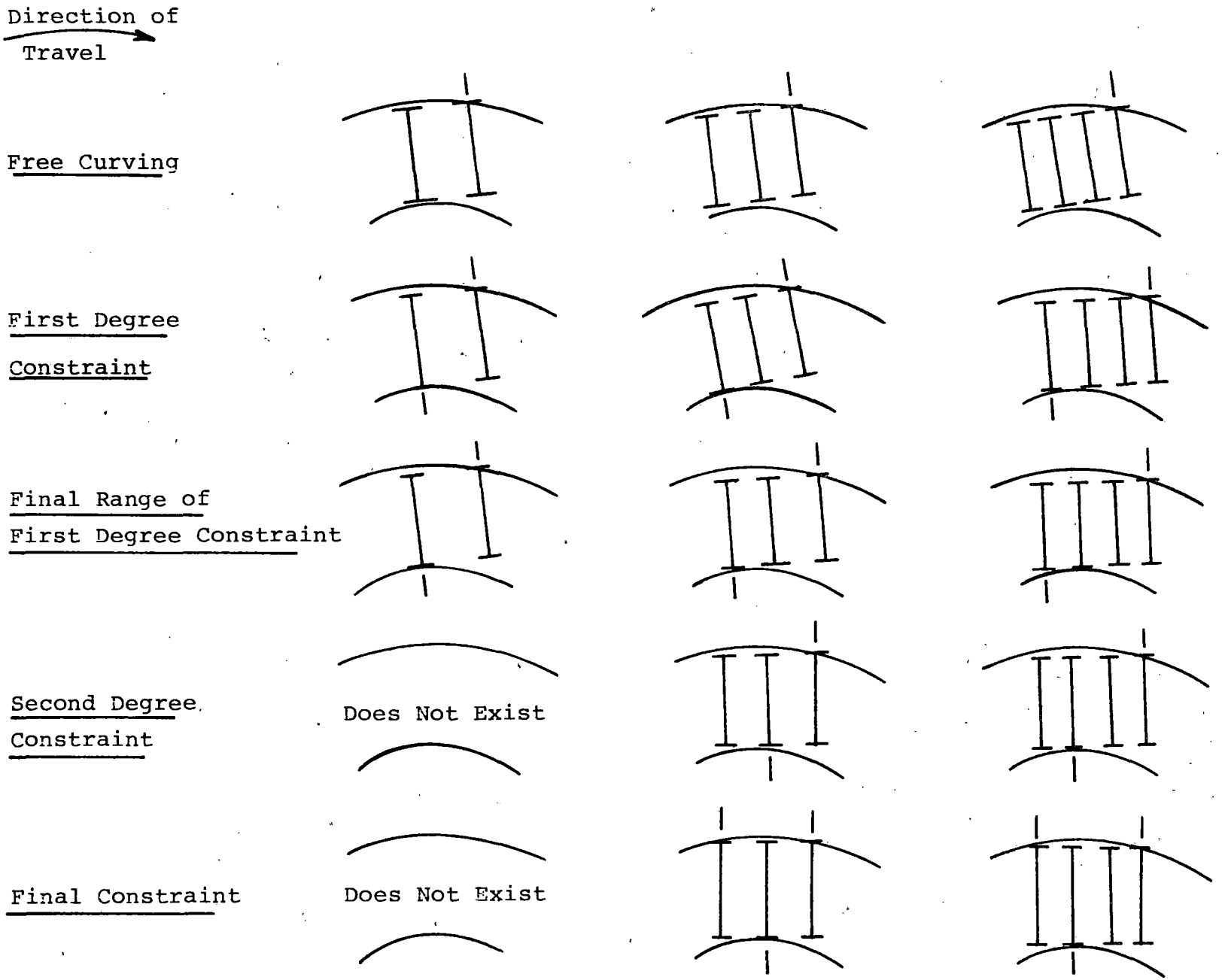

NOTE: Marks indicate flange contact.

FIGURE 3

rail. For a 3 or 4-axle truck the second outer wheel may or may not be in flange contact dependent on the design parameters mentioned in free curving condition. It is generally desirable to have a middle axle flange contact on as sharp a curve as possible due to its causing a reduction of the leading outer wheel flange force.

3.3 Final Range of First Degree Constraint

This range is exemplified by the same location of the wheels with respect to the track as in the first degree constraint; however, the truck frame is beginning to shift with respect to the axles. The truck frame shift manifests itself as a decrease in the axle to truck frame lateral reaction at one side of the trailing axle until the frame moves causing the lateral reaction to shift to the opposite side. For a 2-axle truck, the truck frame is oriented such that the lateral reaction (thrust block, or rubber donut load) between the axle and frame is on the outer side at the trailing axle during curving in first degree constraint, and is shifting to the inner side while entering the final range of first degree constraint. In the case of a 3 or 4-axle truck the lateral reaction at the trailing axle is on the inner side while in first degree constraint, and is shifting to the outer side for the final range.

3.4 Second Degree Constraint

What is called second degree constraint is found only in rigid trucks containing 3 or more axles. It is characterized by curving with the leading outer wheel in flange contact with the outer rail and one of the in-board axle sets in flange contact with the inner rail. With the inception of second degree constraint the flange force at the leading outer wheel will begin to increase at quite a rapid pace as the radius of curvature decreases.

3.5 Final Constraint

Final constraint, as in the case of second degree constraint, occurs only in trucks with 3 or more axles, and as its name implies is the last commonly considered curving mode. In final constraint the truck has reached the limit of its curving capability for, as depicted in Figure 3, the truck has 3 wheel flanges in contact with the rail and can accommodate no further reduction in radius. In the case of the 3-axle truck, flange contact occurs at the leading outer, middle inner, and trailing outer wheels. With a 4-axle truck in final constraint the leading outer, third inner and trailing outer wheel flanges will be in contact with the rail.

3.6 Forced Constraint Modes

Thus far we have been considering constraint modes that are encountered primarily due to curving at no

or limited interaction with the carbody; however, lateral center plate loads encountered in buff or operation at greater than balance speed along with longitudinal loads generated from tractive or braking effort serve to reposition or force the truck into or out of the various constraint modes. For example, a large lateral center plate load acting radially outward with respect to the curve may move the truck from a first degree constraint mode into a free curving position, and similarly a negative lateral center plate load may move the truck from free curving into first degree constraint. Typically, when a truck is influenced by external loads into a different curving position, that constraint mode is called forced free curving, etc.

4. EXTERNAL LOADS & REACTION FORCES

In section 2, the friction forces occurring between the wheel and rail were derived and shown acting as in Figure 2. These forces may be referred to as internal forces as they are generated within the system as a function of pure curving, as opposed to external and reaction forces which are the results of actions occuring outside of the system and those loads requiring to keep the system in equilibrium, respectively. It is these reaction forces occurring between the wheel and rail that we are seeking, for they determine the outcome of curve negotiation.

4.1 Reaction Forces

The reaction forces that have been spoken of are in essence the lateral flange forces that develop between the wheel and rail. These loads along with the friction effect are depicted in Figure 4, with the K's denoting the flange reaction and the F's, the friction force. It is apparent that the longitudinal component of the friction force acting at each wheel will, for the orientation shown, have the tendency to rotate the truck about a vertical axis or point, the friction center. The lateral components will displace the axles laterally until they are constrained by either the truck frame, developing a thrust block load, or by the rail, in which case a flange force develops. The flange reactions that

result are those required to maintain lateral and rotational equilibrium of the truck. Longitudinal equilibrium is maintained by the correct location of the friction center, so that all longitudinal friction components balance. The locations and magnitude of the flange forces that develop are a function of the curve size, truck design, and friction.

4.2 External Loads

Loads from activity occurring externally to the truck may be applied through the center bearing in lateral and longitudinal components, Figure 5. The lateral components have the primary effect of changing the magnitudes and locations of the flange reactions, so that lateral equilibrium will be maintained. In the process, the truck may shift to a different curving constraint mode as mentioned in Section 3.6 to attain equilibrium. The application of a longitudinal load component to the center bearing has the primary effect of shifting the location of the friction center laterally with respect to the truck centerline, so that the longitudinal components of the friction force may now balance the input. Of course, this will result in a redistribution of the lateral flange reactions.

FLANGE AND FRICTION FORCES

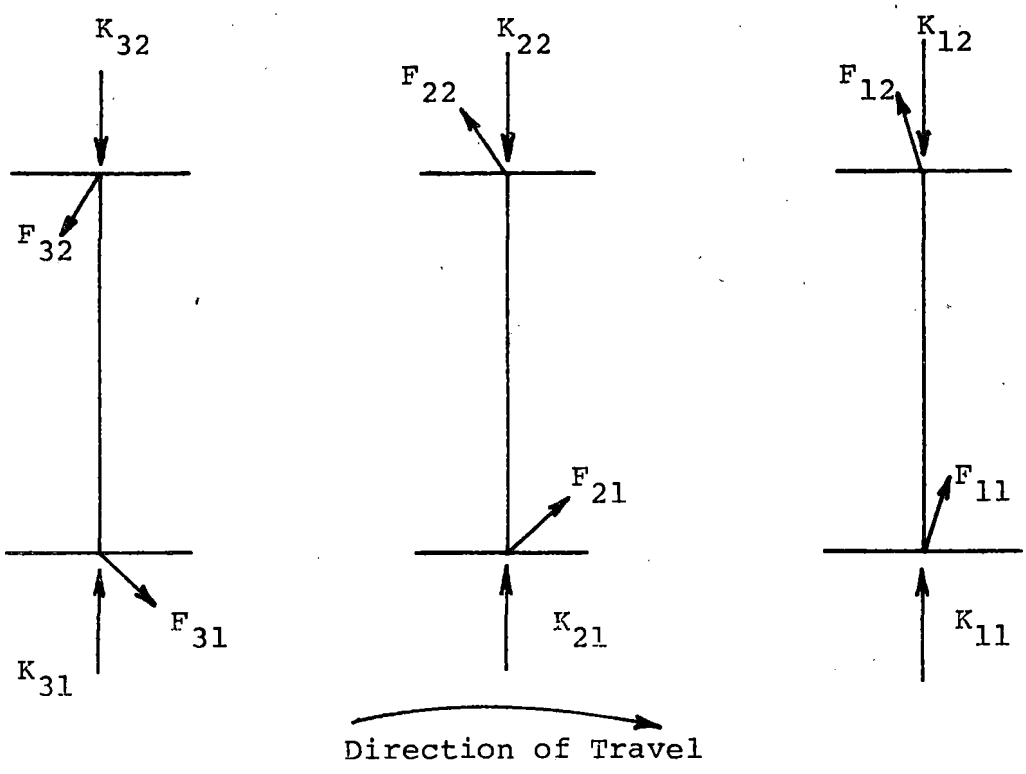

FIGURE 4

EXTERNAL LOADS

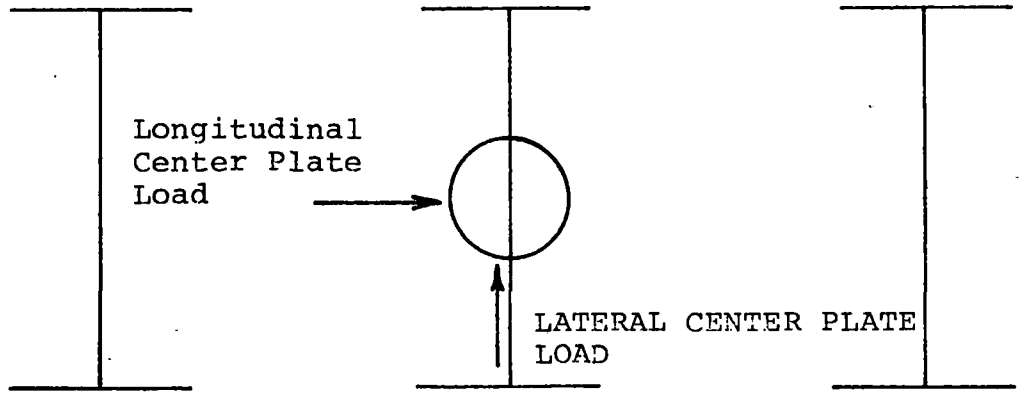

FIGURE 5

5. TRUCK MODEL

The truck is modeled as a rigidly framed set of axles. By rigidly framed it is meant that the two side frames are fixed to one another solidly so that no rotation, parallelogramming, or other relative movement may occur between them. The axles are mounted within the frame such that only lateral movement of the axle with respect to the frame is allowed. This, then, ensures that no rotation about a vertical axis will occur between the individual axles. Each axle is joined to the frame by its lateral journal box suspension only, which consists of a free clearance followed by a spring, see Figure 6. The free clearance, denoted axle to truck frame free lateral in Figure 6, is in actuality the sum of the clearance between the wearing surfaces of the truck pedestal and journal box. This is for the case of a Hyatt type journal box, whereas for a Timken type cartridge bearing it is the clearance between the truck pedestal and bearing wearing surfaces. The spring represents the stiffness between the axle end and the truck pedestal once the free clearance has been taken up. This is the only lateral connection to the truck frame as the small lateral component of the vertical axle to truck suspension may be lumped into the free clearance and spring. No friction on the wearing surfaces is considered.

There also exists a second area of free lateral clearance, and that is the lateral distance between the wheel flange and

the gauging point on the railhead. The magnitude of this clearance is a function of the gauge widening and rail/wheel wear. The assumption is made that the rail is rigidly fixed to the ground and has no qualities of resilience or deflection.

It is assumed that all tractive effort, braking effort or buff forces are reacted at each individual wheel as a function of the individual vertical load acting on the wheel, and that each truck reacts one-half of the total amount applied to the locomotive. Also assumed is that all effects of the spin creep reacting at each wheel are small enough in comparison with other considerations to be neglected.

As a final consideration, the point of connection between the truck and carbody is modeled to transmit both lateral and longitudinal force components without imposing rotational stiffness of any sort to the truck, in other words, a frictionless pivot. (Provision is made for an initial rotational "breakaway" moment term to be considered. See "Appendix C".

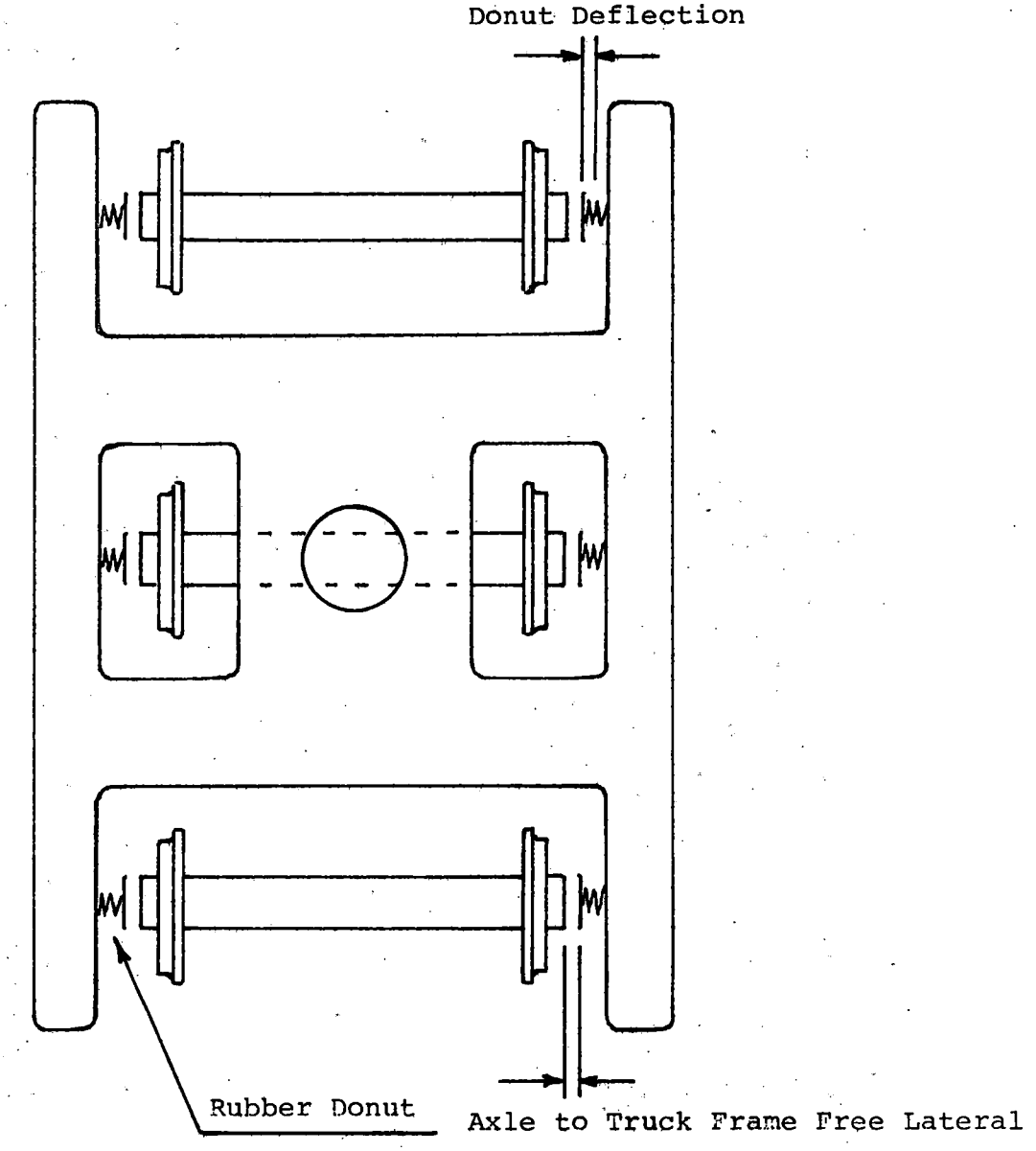

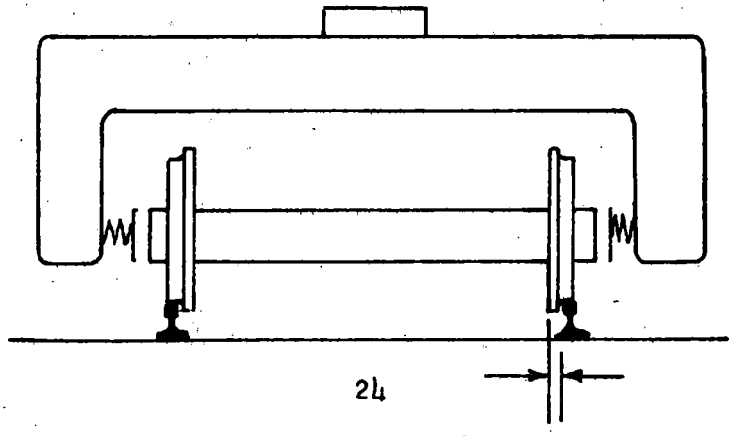

24

FIGURE 6

Rail to Wheel Flange Nominal Clearance

6. METHOD OF SOLUTION

Referring to Figure 4, it can be seen that there are twelve (12) possible reactions between the wheels and rails at any particular instant of time; however, for assumptions made in this model, the number may be reduced considerably. First of all, it is known that for all but very abnormal cases only one wheel of each wheel/axle set will be in flange contact at a time. This eliminates three of the unknowns. Secondly, since the rigid body concept is being used, the frictional forces at each wheel will all be related, so that knowing one or the friction center location will lead to the solution of all. Therefore, the initial concept of the model has been reduced to four unknowns, three flange forces and the friction center location. Three of these unknowns are independent, and the fourth is dependent. At this point, three equations may be written for equilibrium:

$$\Sigma \quad F_x = 0$$

$$\Sigma \quad F_y = 0$$

$$\Sigma \quad M = 0$$

However, a fourth equation cannot be written to locate the friction center, because due to the free clearance between the wheel and rail, axle and truck frame along with the deflection of the rubber donut due to the combined action of the friction and flange forces, no geometric solution can be written. So, with three equations and four unknowns the

problem has become statically indeterminate. In order to solve this problem, a numerical analysis technique which incorporates an iterative method and convergence routine must be employed. The iterations and convergence are done on the longitudinal location of the friction center. (The lateral location of the friction center is a function of vertical wheel loads and the longitudinal center plate load, and once a longitudinal friction center location has been established the lateral location may be easily found to react the longitudinal input.)

As an initial step, it must be determined into what curving constraint mode the truck would be for the particular size curve given if there were full deflection of the rubber donuts. This may be done by computing the transition point, as a function of curvature, between free curving and first degree constraint. If the radius of curvature being considered is greater than the transition curvature, it may be assumed as an initial starting point that the truck is in free curving, and in first degree constraint if the curve size modeled is less than the transition curvature. A similar procedure may be used to determine if the truck is in second or final constraint.

In order to locate the transition radii (free curving to first degree constraint, first degree constraint to second degree constraint, etc.), a geometric relationship is introduced to calculate the longitudinal friction center

location as a function of curvature. This may be done with the assumption of full donut deflection and knowing that at the inception of first degree constraint the trailing inner wheel has come into flange contact with the rail, however, its reactions or K31 must be equal to zero. Figure 7 depicts the truck position and variables X, Y and Z. From experience it is known that the reactions occurring between the axles and frame in first degree constraint are located at the leading and trailing inner positions and the middle outer position. With this, the position of the wheels with respect to the rails and the axles with respect to the truck frame are known and the longitudinal friction center location may be established. Recall that for equal wheel loads and no longitudinal center plate loads the friction center is located on the centerline of the track as its velocity must match the vehicle velocity.

The centerline of the truck frame at each axle may now be calculated at a distance (X, Y or Z) from the center of curvature for the constraint modes. In free curving only, the leading axle may be geometrically located.

$$X = R + \varepsilon_1 + e_1 + \delta_1 \qquad (1)$$

Where: R = Radius of the Curve

ε_1 = Wheel to Rail Free Clearance at Axle 1

e_1 = Axle to Truck Frame Free Clearance at Axle 1

δ_1 = Deflection of the Rubber Donut at Axle 1

In the first degree constraint, the truck centerline may be located at both the lead and trailing axle positions:

$$X = R + e_1 + \varepsilon_1 + \delta_1 \tag{2}$$

$$Y = R - \varepsilon_3 + e_3 + \delta_3 \tag{3}$$

With this assumption of a maximum deflection of the thrust block, the distance from the leading axle to the friction center, D1 may be determined by:

$$X^2 - D1^2 = R^2 = Y^2 - (WBASE - D1)^2 \tag{4}$$

$$X^2 - D1^2 = Y^2 - (WBASE^2 - 2D1 \cdot WBASE + D1^2)$$

$$D1 = \frac{X^2 - Y^2 + WBASE^2}{2 \cdot WBASE} \tag{5}$$

This now enables calculation of the friction-creep forces at each wheel. The flange force at the trailing axle may be found through the force, moment equilibrium equations. At this point an iteration procedure commences by varying the radius until the value of K31 approaches zero, at which point the transition from free curving to first degree constraint has been located. With the truck position known (free curving, first degree constraint, etc.), the system may now be solved for the exact radius and set of conditions given. In free curving the friction center is iterated until equilibrium is maintained without flange contact at the trailing axle and geometric compatibility is satisfied. For first degree constraint the friction center location is calculated by equation (5) using for the deflection of the donut the loads resulting from the previous iteration. This

is continued until the friction center calculation converges to a constant value at which point equilibrium has been maintained. Finally, the computed value of the donut deflection is compared to the assumed value used in the transition from free curving to first degree constraint calculation. If they are different, the newly computed value is used as the assumed value and the entire process is repeated until the calculated result approaches the assumed value. At this point, both force equilibrium and geometric compatibility have been maintained and the truck has been successfully modeled. A similar procedure is followed to model the truck in the other constraint modes.

6.1 Intermediate Axle (3, 4-Axle Trucks)

For an intermediate axle with the truck in free curving, first degree, or other forced constraint mode the flange reaction with the rail is computed independetly of the summation of force, moment equations which are used to obtain the leading and trailing axle flange forces. For a 4-axle truck there are two intermediate axles that may be in flange contact with the rail. The friction force acting on the wheelset results in a lateral displacement of the assembly until it is either constrained by the rail, truck frame, or both. If the free clearance between the axle and truck frame is great enough, the wheel flange will move up against the rail and the flange force reaction will be given as:

$$K_{YX} = f_{Y1} + f_{Y2}$$

Where f denotes the lateral component of the friction developed at each wheel of that particular wheel/axle set. For this condition the wheel/axle set is commonly referred to as externally guided. If the clearance is not great enough, the axle will come in contact with the rubber donut and begin to compress it. In so doing, the additional lateral motion gained may allow the wheel to move up against the rail, in which case the flange reaction would be:

$$K_{YX} = f_{Y1} + f_{Y2} - k\delta$$

Where k is the stiffness of the rubber donut and δ its deflection. Once the maximum deflection of the donut has been attained with no flange contact at the wheel, the friction force is reacted entirely by the truck frame. In this case the axle set is said to be internally guided, and the friction force transmitted into the truck frame will be reacted at some other wheel.

GEOMETRIC CONFIGURATION

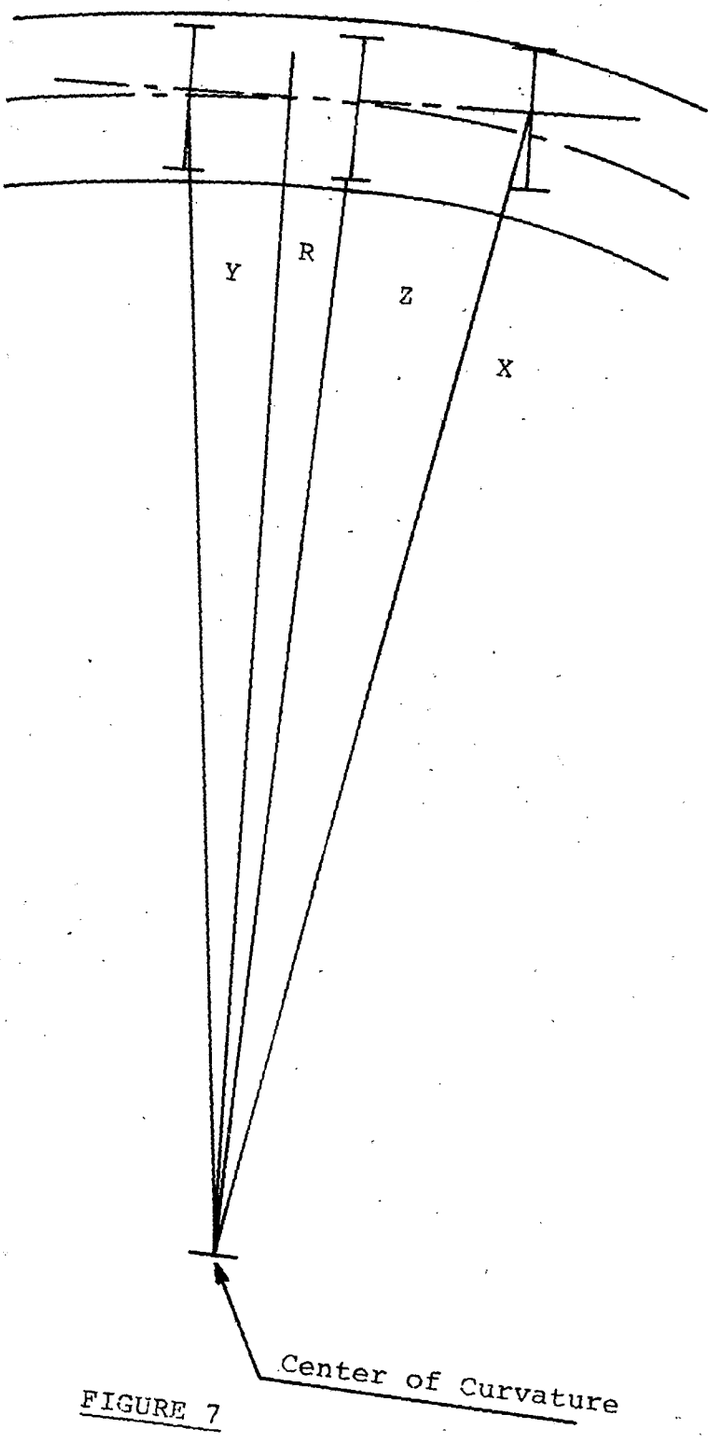

FIGURE 7

7. Results

The primary interest in curve negotiation is focused on the flange or guiding force at the leading outer wheel of the truck, as this is the most highly laterally loaded wheel during normal curve negotiation. It is, therefore, of great consequence how operating practices and design parameters affect the lateral loading of this wheel if not from the derailment standpoint, then from wear considerations. The quantity that provides an index to evaluate the wheel climb, rail rollover, or wearing tendency is referred to as the net lateral load. In terms of force, the net lateral load at a wheel is the vectorial sum of the flange force and lateral component of the friction force. This net lateral load is the "L" term in the L/V ratio.

The "standard" truck chosen for comparison purposes, has the following characteristics:

1. Axle to truck frame free lateral clearance at each axle equals $\pm$ 0.1875", or 0.375" total.
2. Free clearance between the wheel flange and rail at each wheel equals $\pm$ 0.340", or 0.680" total per wheel/axle assembly. (New wheels and rail.)
3. The rubber donut has a maximum deflection of 0.250" and may be modeled as a linear spring with a rate of 20,000 lbs./inch.

Note, that in all cases the graphs are drawn for a truck curving with no lateral or longitudinal center plate loads unless noted. This is analogous to the case of a locomotive

traversing a curve at balance speed with no buff, tractive, or braking efforts developed.

Figure 11 indicates for a 3-axle truck the effect of increasing the axle to frame free lateral at the center axle in steps of 1/8" per side. It is apparent that the additional lateral allows more load to be taken at the rail rather than being reacted by the truck frame. This results in a decrease of the net lateral load at the guiding wheel which can be substantial on the sharper curves, 8% on a 6 degree curve. It may also be noted, that except for the truck with 7/8 free lateral at the middle axle is partially constrained in all other cases.

Figure 12 indicates the effect of increasing the lateral at all axles equally. Much the same behavior is noted as with increasing only the center axle lateral, however, it is much more pronounced in its effect on the middle axle flange force. For a truck with 5/8" lateral at all axles the center axle is externally guided up to 2-1/4 degrees of curvature, and up to 4 degrees for a truck with 7/8" total lateral clearance. This again results in a reduction of the leading axle net lateral load.

Next to be evaluated is the importance of wheel to rail clearance and the effect of gauge widening on the tracking of a truck. Figure 13 depicts how gauge widening of 1/2" total changes the net lateral loads. As long as the truck is in free curving, the addition of wheel/rail clearance will

not change the curving forces since the truck will follow the outer rail. However, when in first degree constraint, the addition of gauge widening will allow the truck to skew to a greater degree within the rails resulting in an increase in the friction and flange forces as the angle of attack rises. The true benefit of gauge widening is in its pushing of second degree and final constraint to lower radii of curvature, but in first degree constraint curving it can be very detrimental, and ineffective for free curving.

The effective spring rate of the rubber donut is another truck design parameter that may have a bearing on the curving activity of the truck. It can be seen in Figure 14 that the rubber donut stiffness has a slight effect on the net lateral loads generated during curving and that, in general, the softer the donut the better. It is obvious that a less stiff donut will allow greater lateral displacement of the middle axle allowing it to react more of the friction component against the rail. This again is beneficial to the guiding force at the leading outer wheel.

The friction-creep relationships presented in Section 2 are the heart of the truck curving model, for it is the friction force developed between the wheel and rail that must be reacted by the flange force. It is, therefore, essential that an accurate friction versus creep relationship be available for the situation being modeled. However, it is indeed a very difficult, if not impossible task to predict a relationship for a specific situation, so it must be known how minor changes in the friction-creep curve will

affect the outcome of the model. Figure 15 depicts how the friction relationships shown in Figure 16 change the output of the model. It can be seen that the model is very sensitive to the shape and slope of the assumed friction curve and that quite an error may be introduced by the use of an inaccurate relationship. It should be noted that Curve 1 in Figure 16 is the result of extensive field testing conducted by Electro-Motive Division, GMC.

The effect of lateral center plate loads on curving forces may be seen by examination of Figure 17. As the center plate load increases, the truck is being pushed up against the outer rail and the friction center moves toward the center of the truck. With the truck displaced laterally as much as possible, the friction center will be at the geometric center of the truck, accounting for the very low net lateral loads at the middle axle. The leading and trailing outer wheels will divide and react the center plate load at the rail. As the curve becomes sharper, the load is not great enough to hold the truck against the outer rail and it starts to slip into a forced free curving condition. This moves the friction center farther away from the lead axle increasing the frictional component, hence flange reaction at the second outer wheel. The middle axle, however, remains externally guided on sharper curves than normal as the truck is disposed toward the outer rail by the center plate load.

Figure 18 depicts the relationship of the flange forces on a 3-axle truck, with first degree constraint beginning at about a 6 degree curve. The effect of free clearance within and external to the truck on the point where first degree constraint becomes less pronounced and that with gauge widening of 1.2" it plays no role at all for normal ranges.

The type of journal bearing employed in the truck plays a role in the tracking of the truck as evidenced by Figure 20, which compares a typical cartridge type bearing with the basic model bearing. It may be observed that there is a significant difference in the behavior of the trucks with the two types of bearings, especially in that the cartridge bearing truck reaches second degree constraint while while on the same size curve the truck with model bearings remains in first degree constraint. This is due to the cartridge bearing design which does not incorporate any lateral axle suspension that would be able to deflect and allow additional clearance that would keep the truck in first degree constraint.

Figure 21, 22, and 23 indicate that for a 2-axle truck, unlike a 3-axle truck changes in axle free lateral, rail to wheel clearance and the stiffness of the rubber donut have little effect, if any, on the net lateral loads in the normal curving ranges. This is due to the fact that the truck is in first degree constraint in this range, so it is tracking with one wheel only in flange contact. In fact, this wheel

does not generate greater than 0.008 radians creep as evidenced by Figure 24, where the same results are obtained up to a 16 degree curve with the use of both friction-creep Curves 1 and 2 (Fig. 16).

The net lateral loads for a 4-axle truck are plotted in Figure 26, which indicates that on a 4 degree curve first degree constraint is entered and on a 12 degree curve the truck reaches second degree constraint. The net lateral load at the leading outer wheel for the 4-axle truck is shown plotted with the leading outer wheel net lateral loads for the guiding wheel are 48% higher for the 3-axle truck, and 94% higher for the 4-axle truck than the 2-axle truck on a 4 degree curve.

7.1 Validation

Figures 28 and 29 compare typical computer predicted data with the field data obtained through tests at Electro-Motive Division, GMC. It can be seen that there is quite good correlation between computed and measured data, especially when considering the wealth of unknown and assumed parameters such as a linear rubber donut and the average friction creep curve.

It may be noted, that the field data used in the validation curves is the same data presented in ASME Paper No. 65-WA/RR-4 by Messrs. Koci and Marta in 1965.

Figure 11
NET LATERAL LOAD v/s CURVATURE

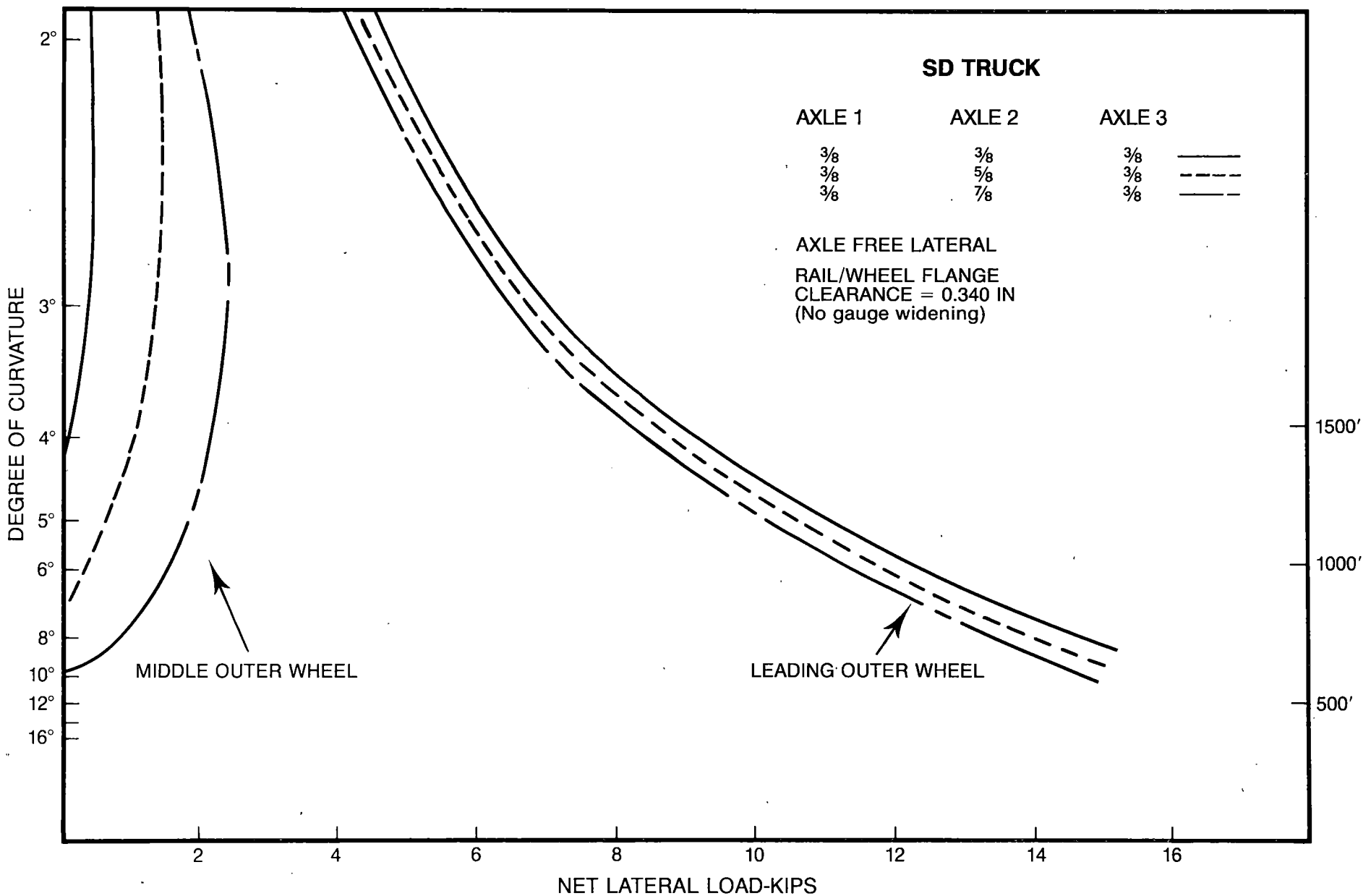

Figure 12
NET LATERAL LOAD v/s CURVATURE

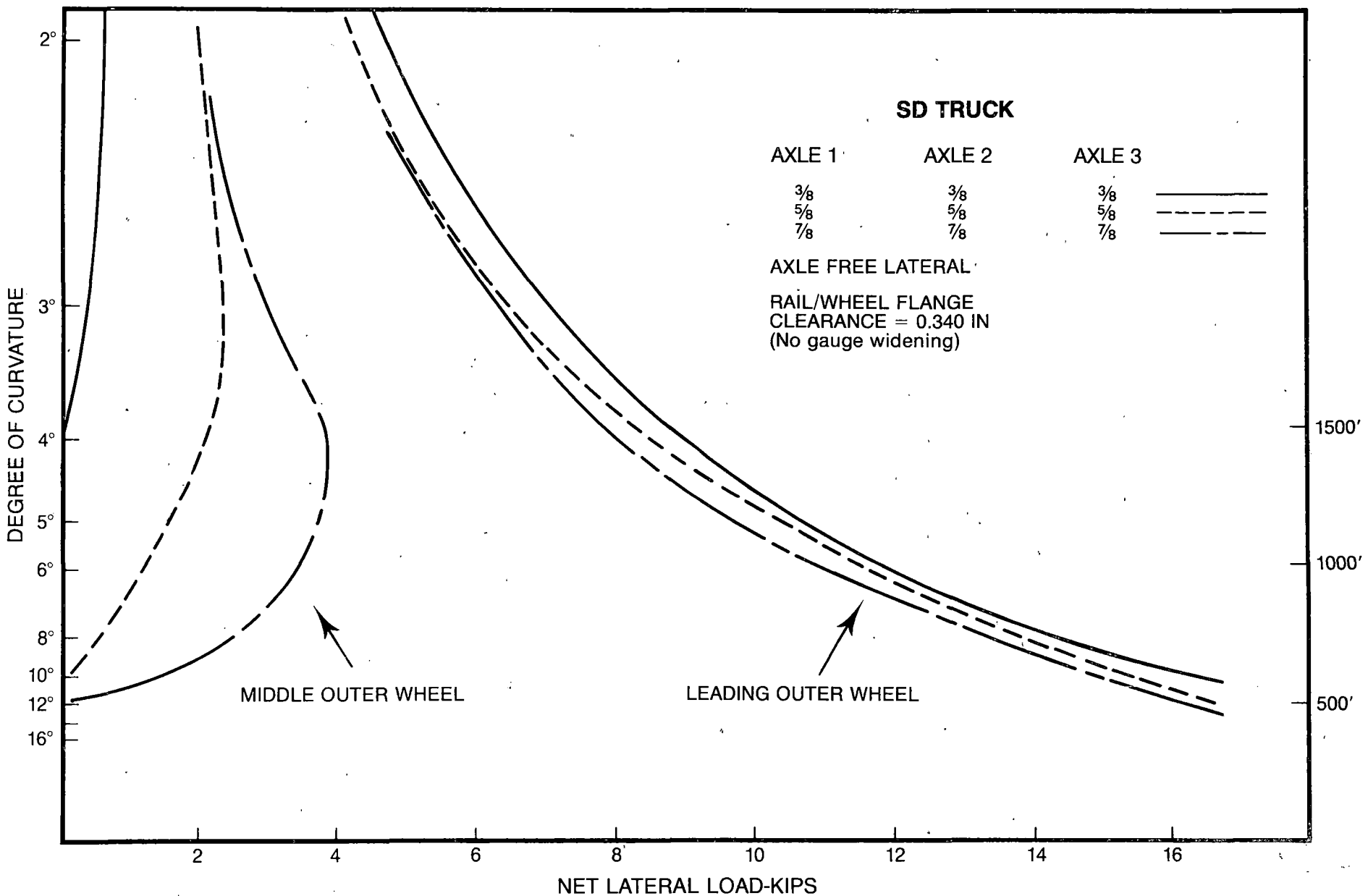

Figure 13
NET LATERAL LOAD v/s CURVATURE

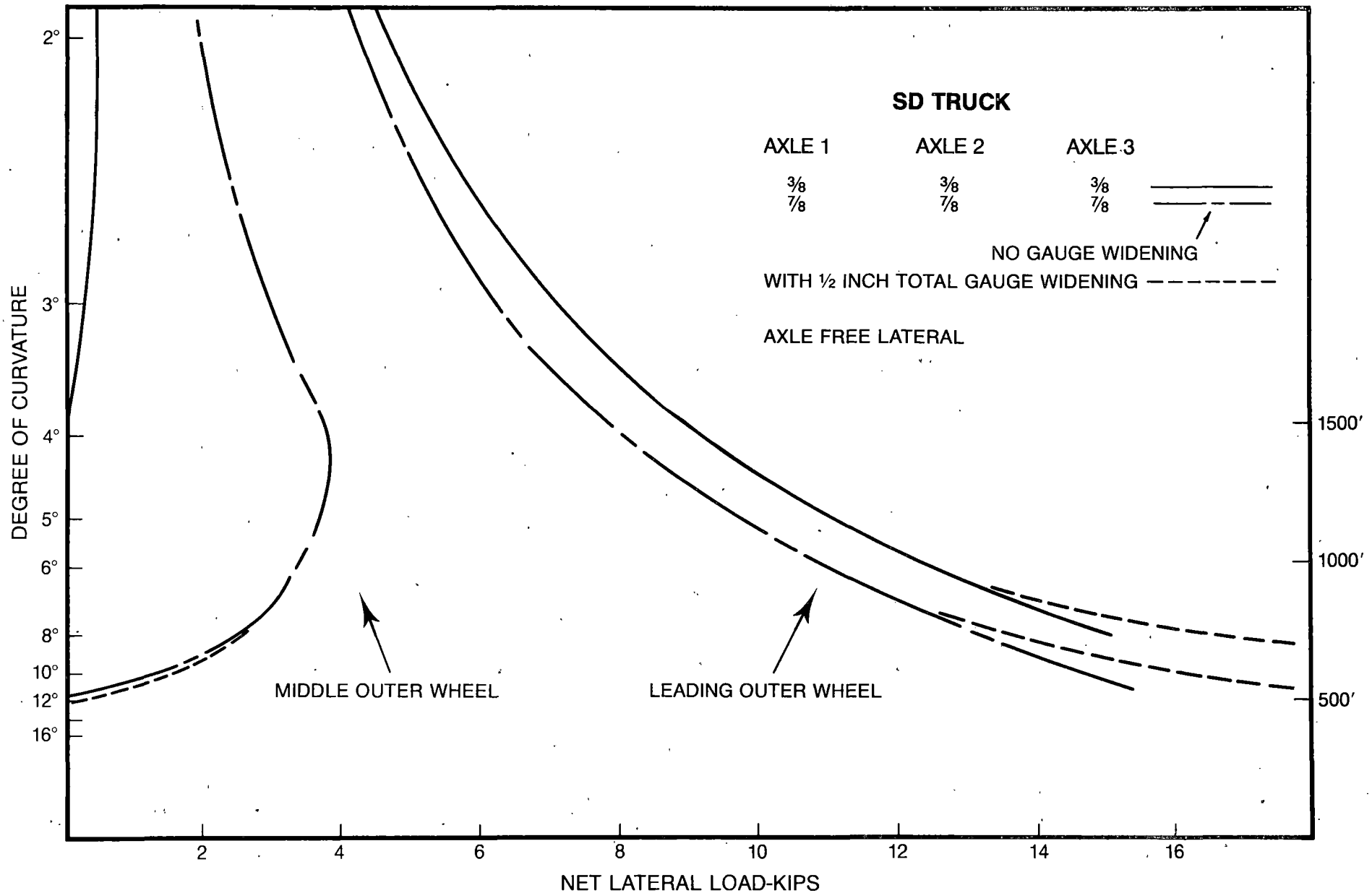

Figure 14
NET LATERAL LOAD v/s CURVATURE

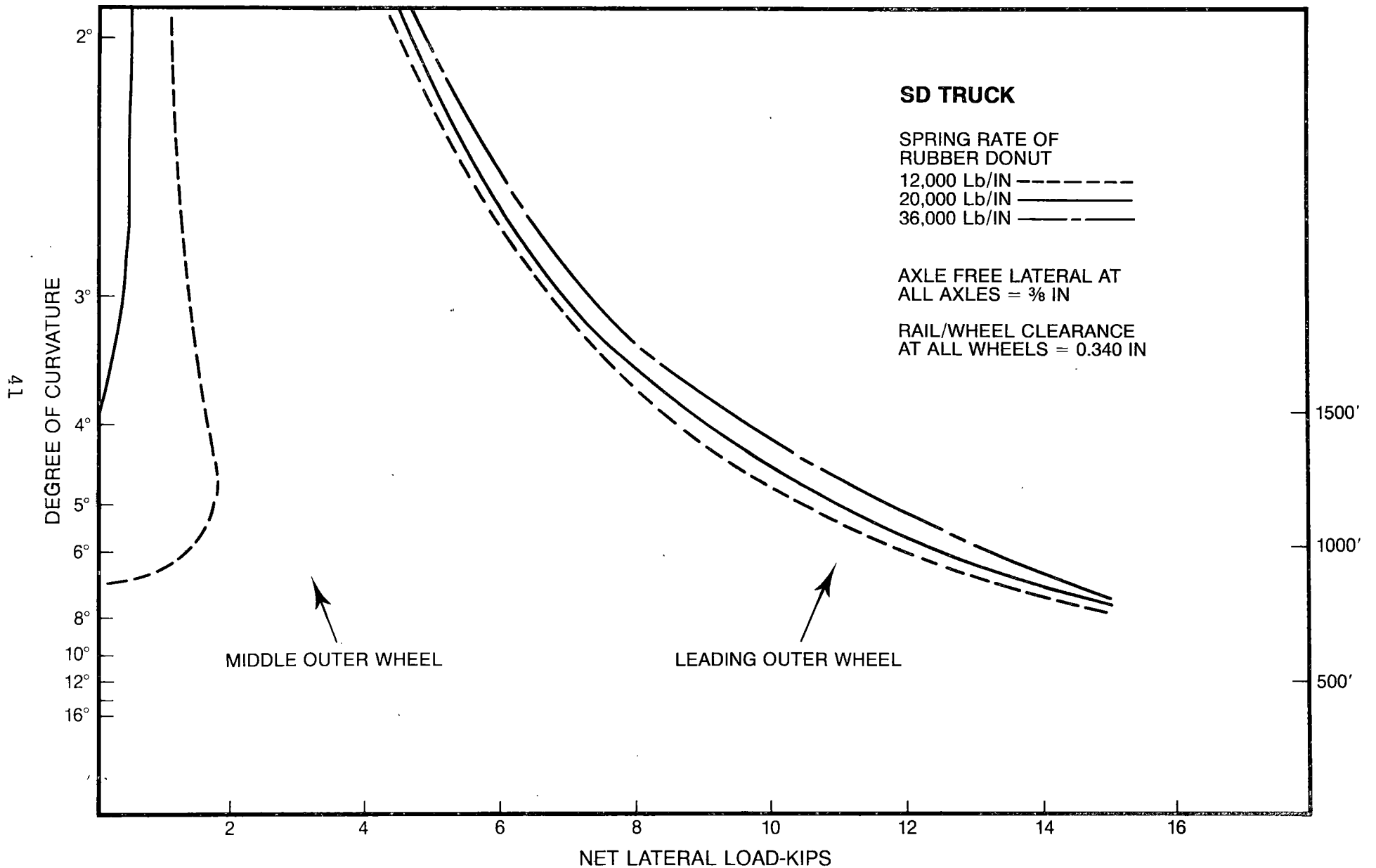

Figure 15
NET LATERAL LOAD v/s CURVATURE

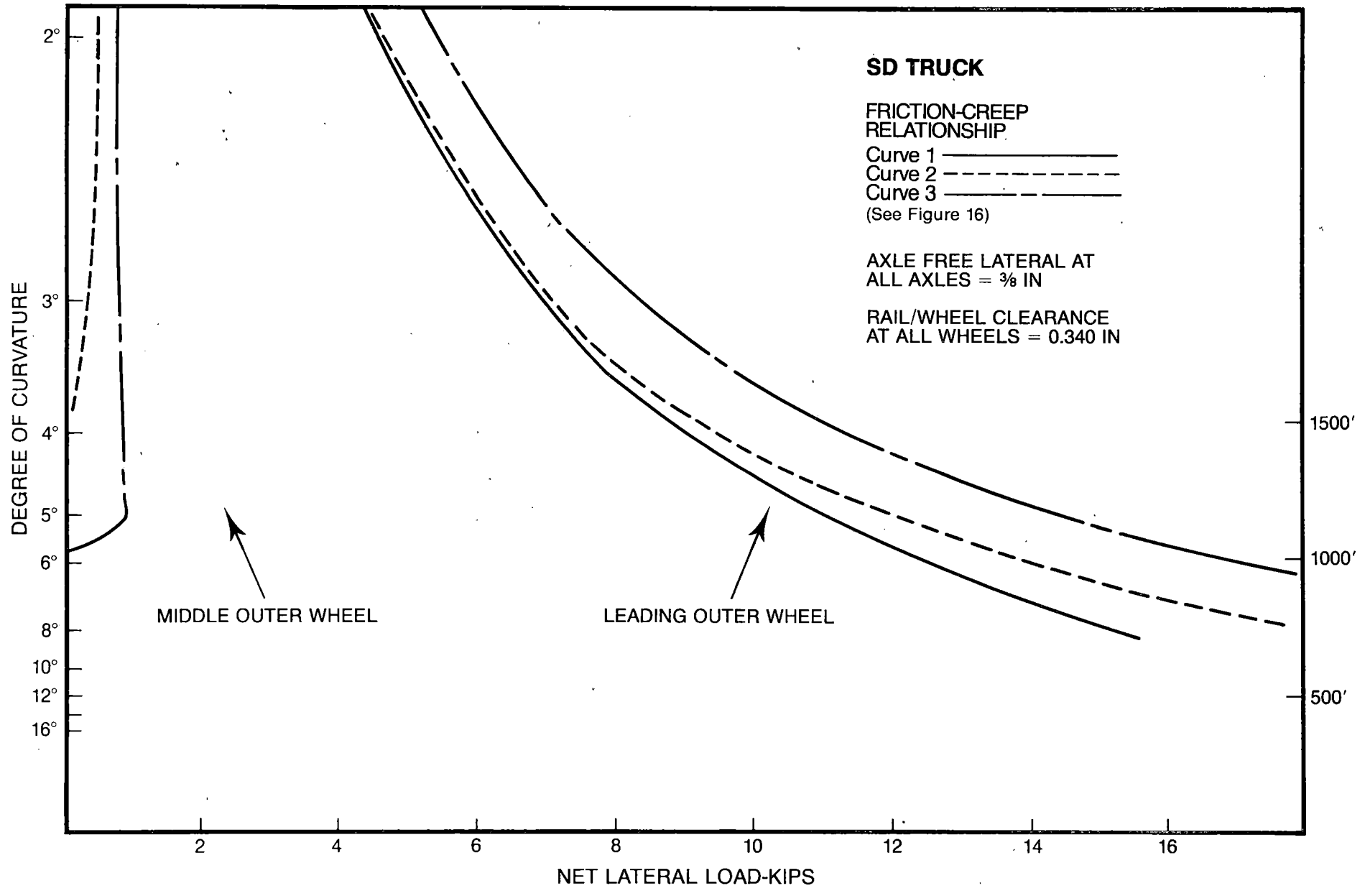

Figure 16
FRICTION-CREEP RELATIONSHIPS

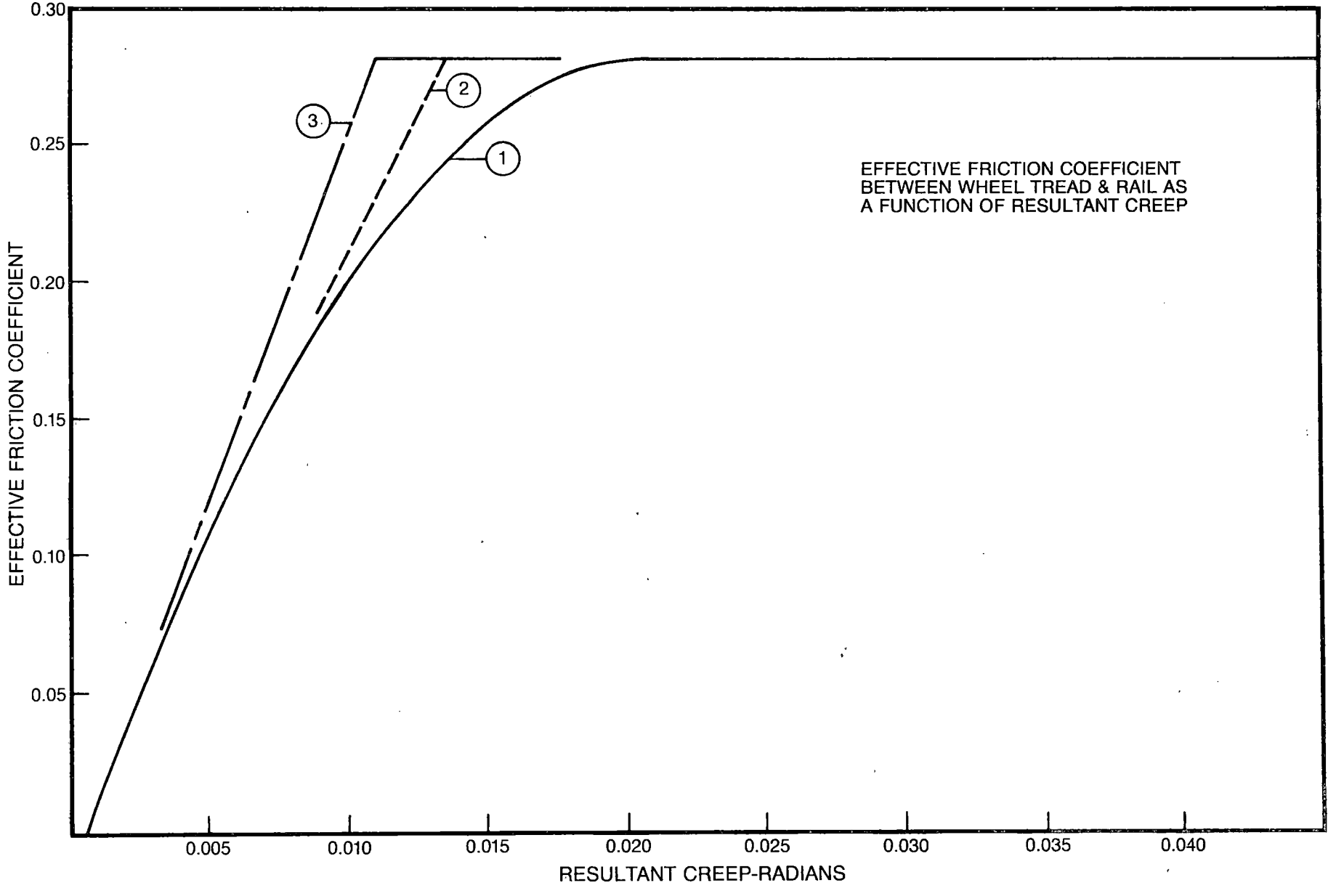

Figure 17
NET LATERAL LOAD v/s CURVATURE

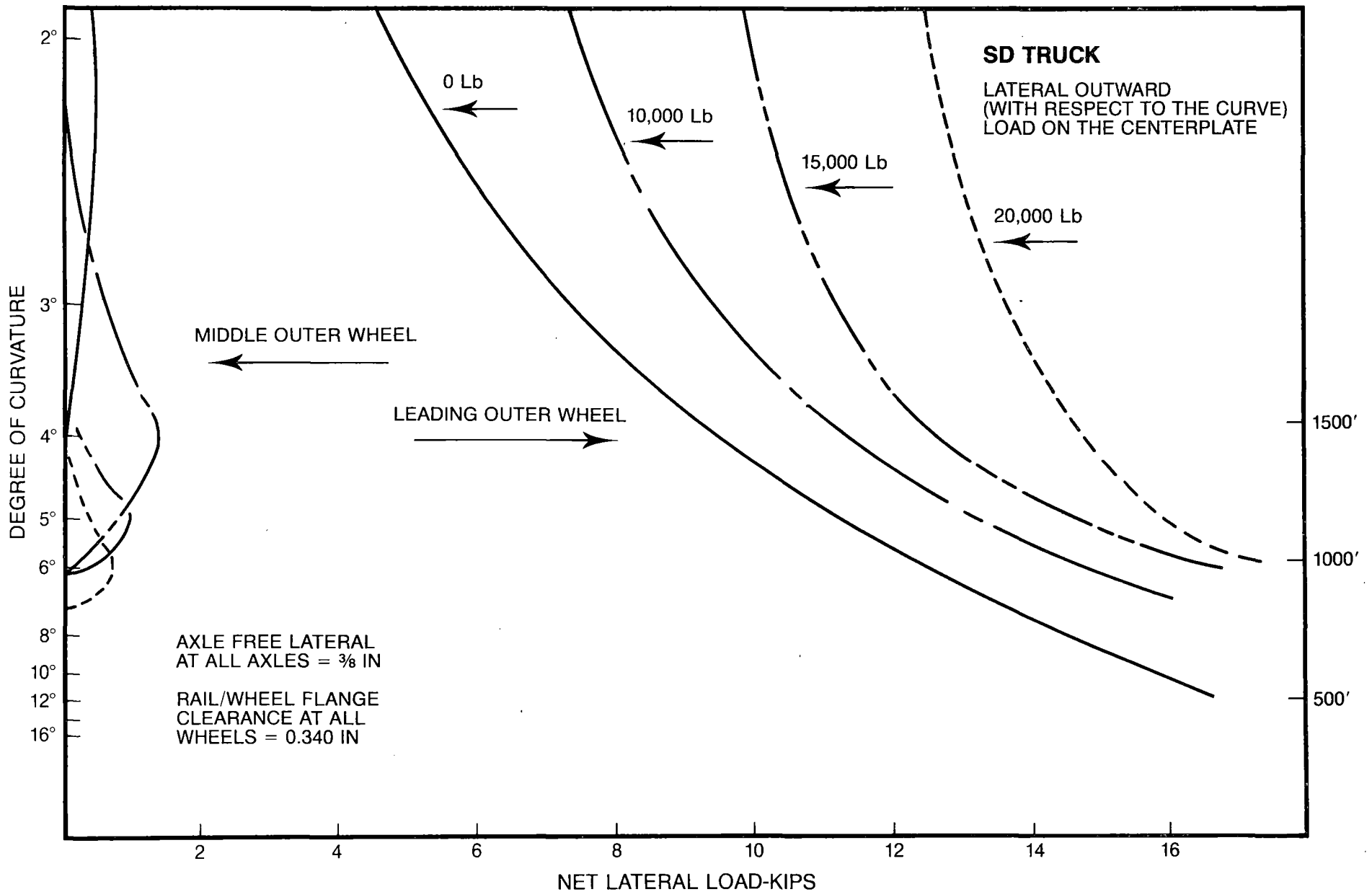

Figure 18
FLANGE FORCE v/s CURVATURE

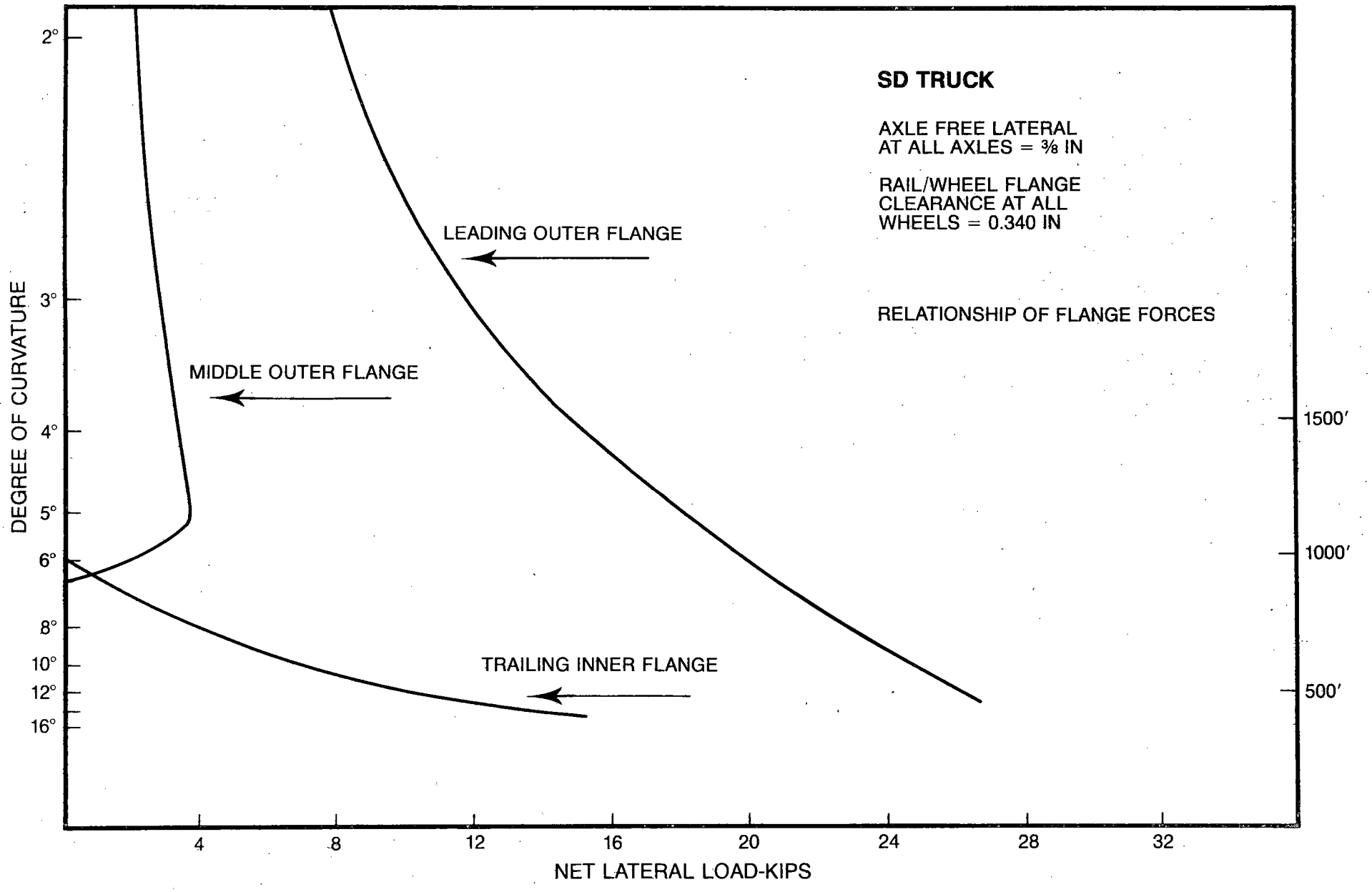

Figure 19
INCEPTION OF FIRST DEGREE CONSTRAINT

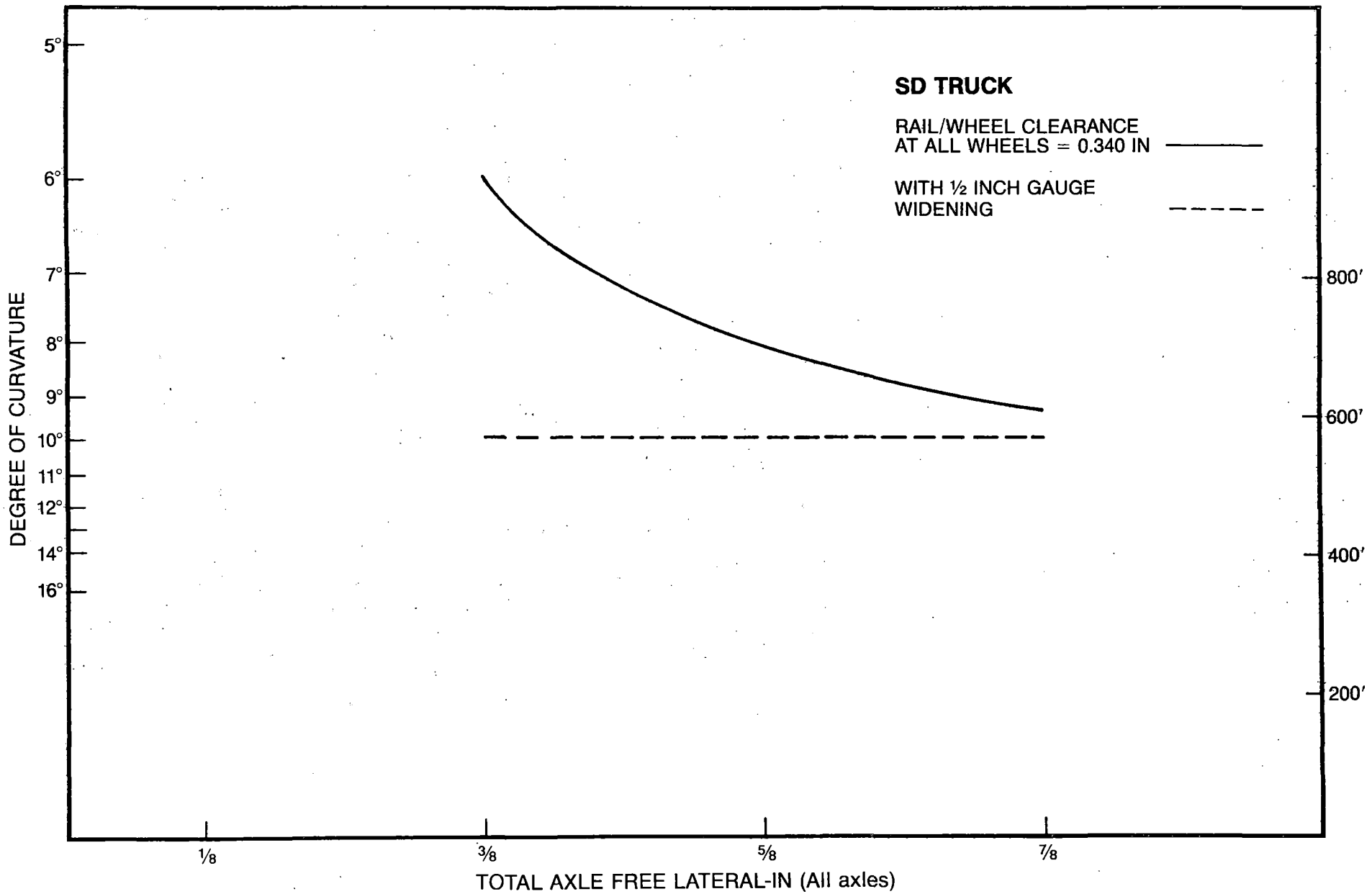

Figure 20
NET LATERAL LOAD v/s CURVATURE

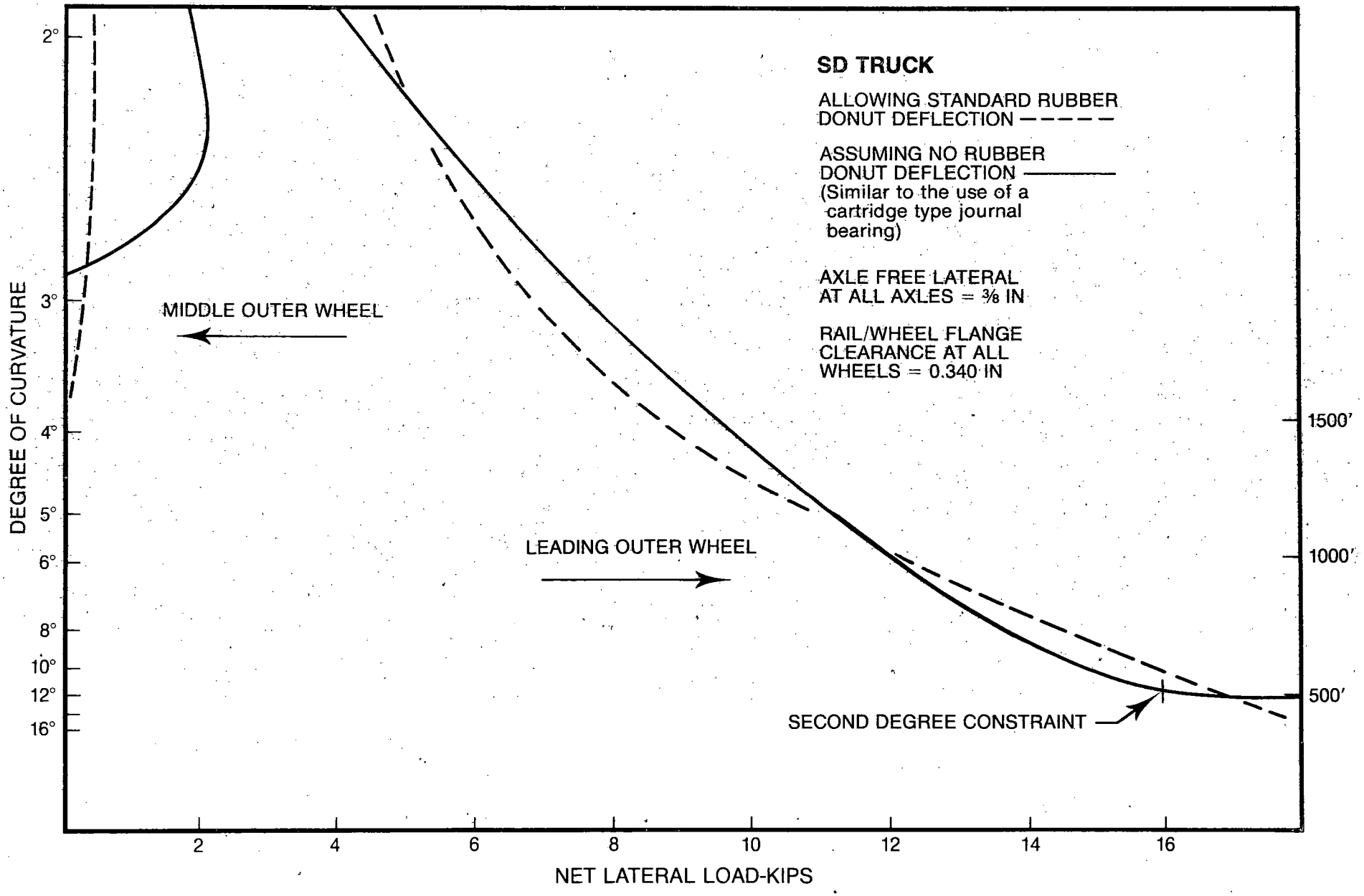

Figure 21
NET LATERAL LOAD v/s CURVATURE

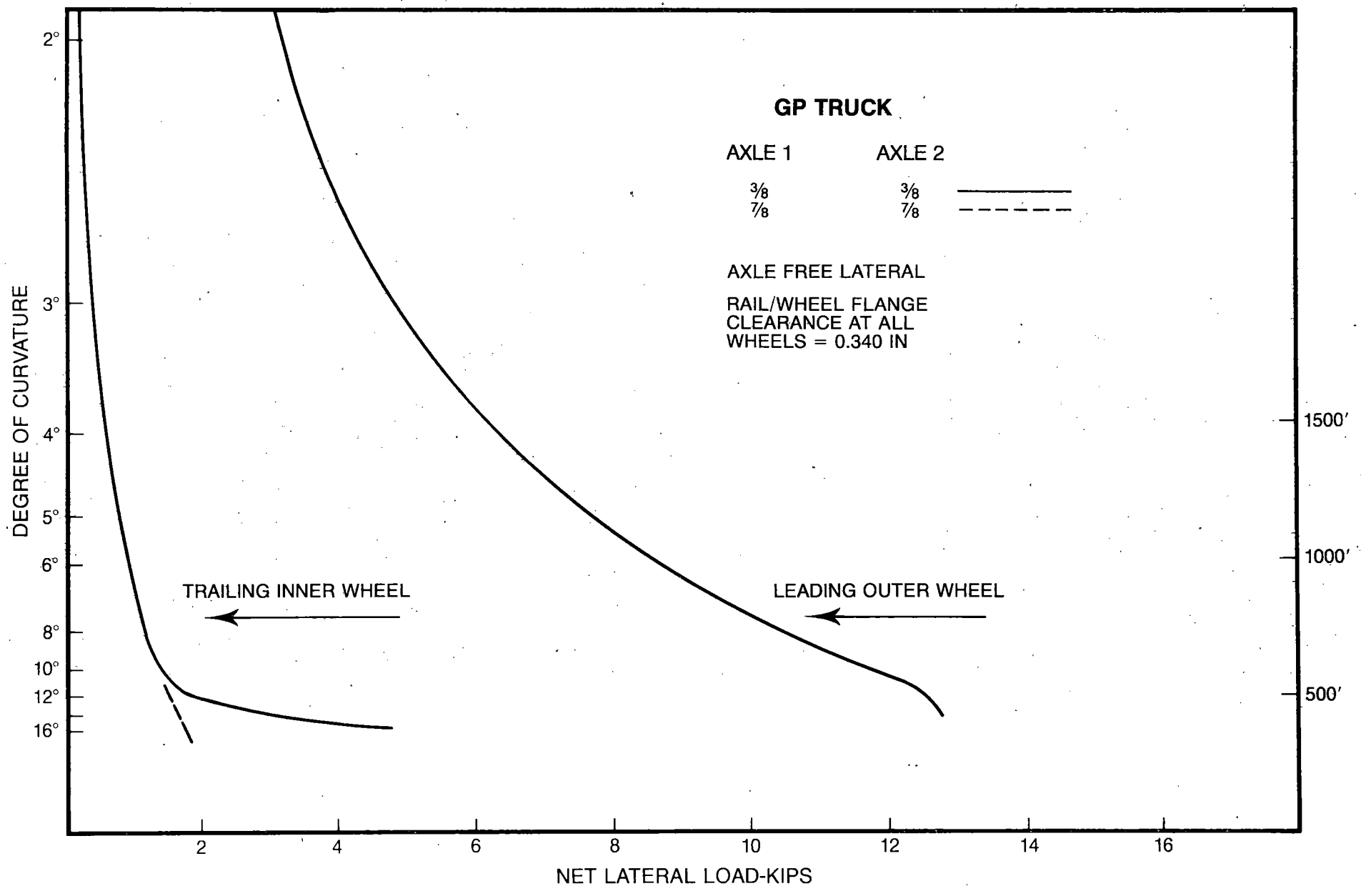

Figure 22
NET LATERAL LOAD v/s CURVATURE

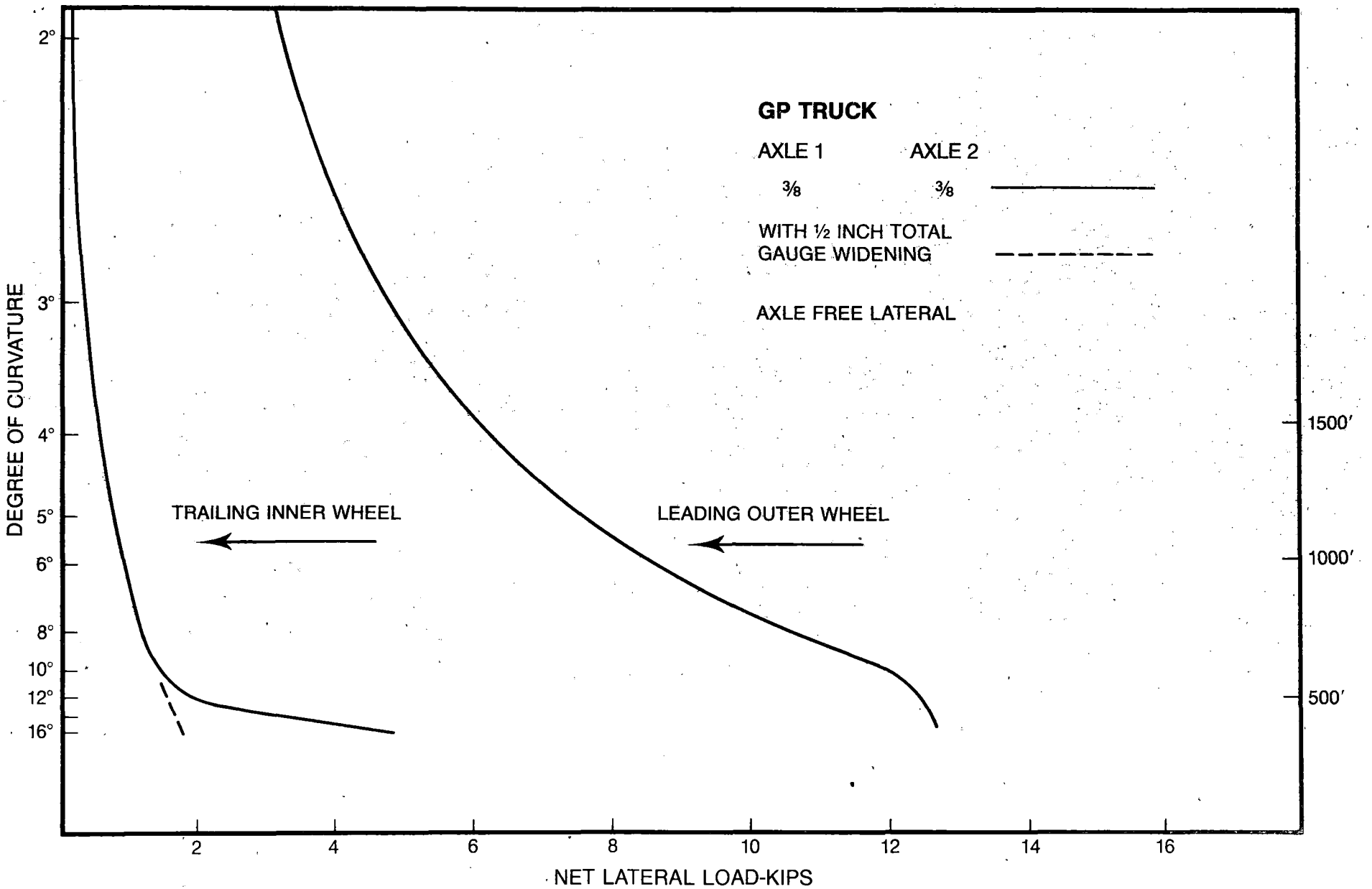

Figure 23
NET LATERAL LOAD v/s CURVATURE

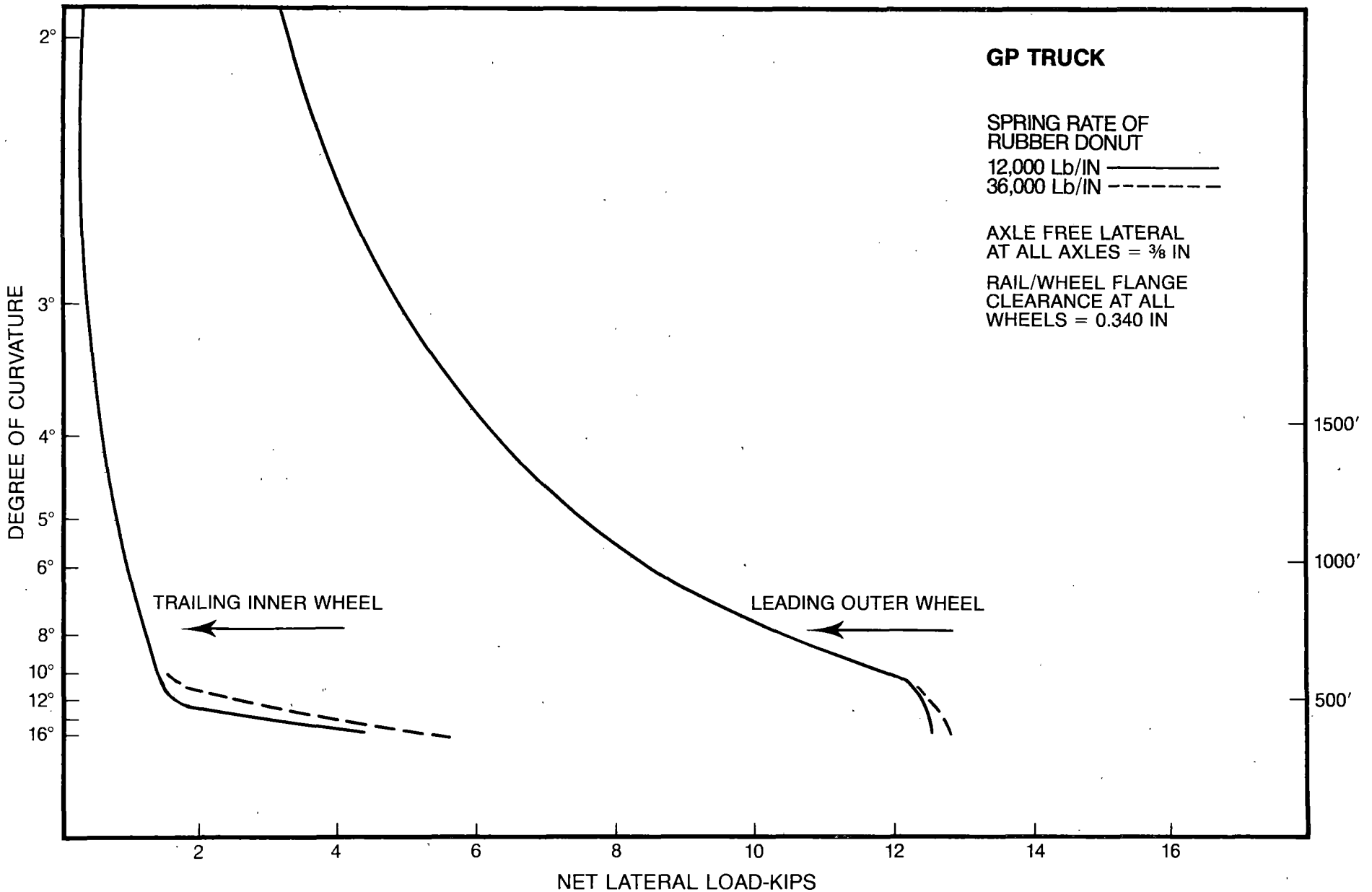

Figure 24
NET LATERAL LOAD v/s CURVATURE

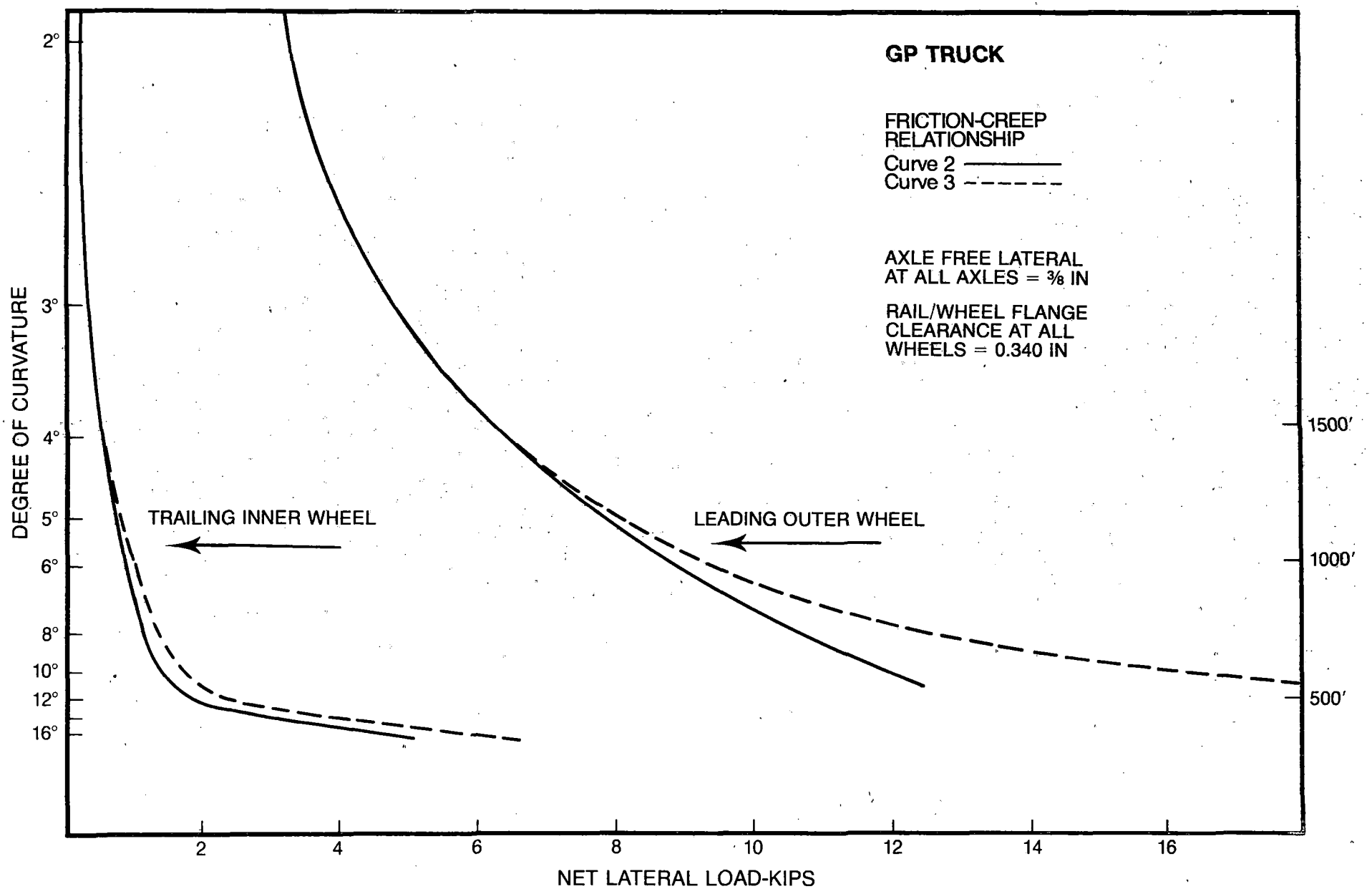

Figure 25
NET LATERAL LOAD v/s CURVATURE

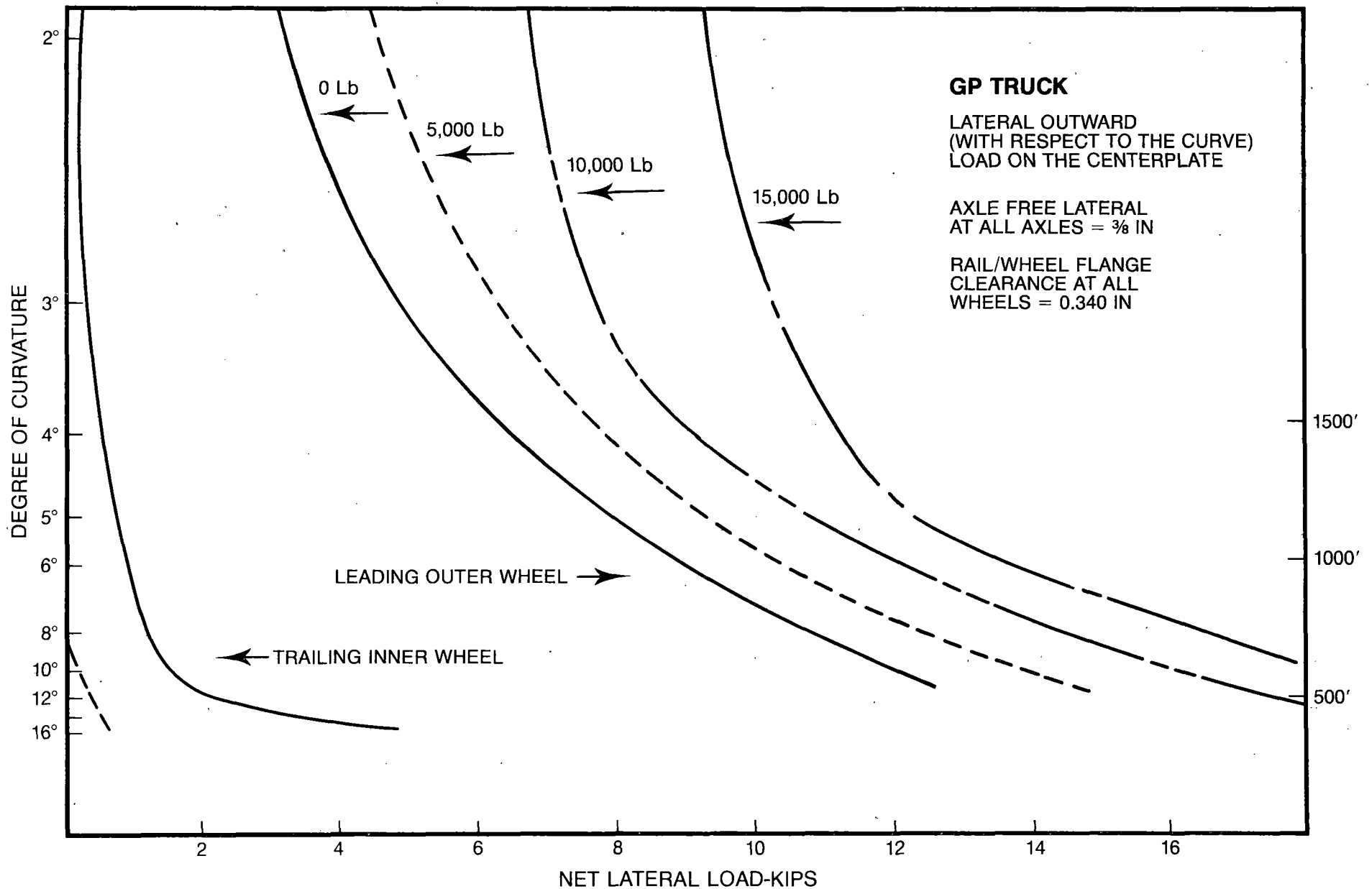

Figure 26
NET LATERAL LOAD v/s CURVATURE

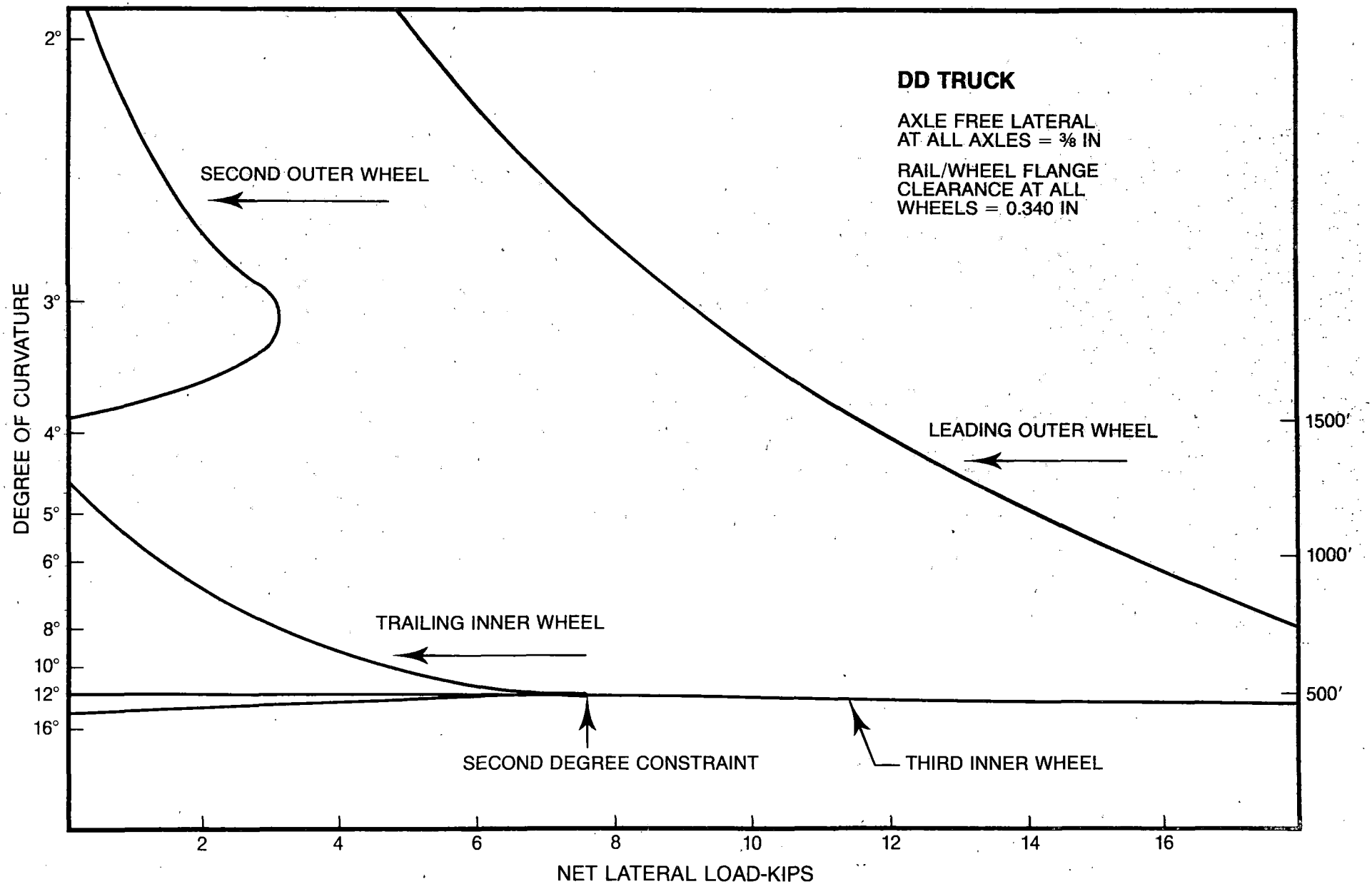

Figure 27
NET LATERAL LOAD v/s CURVATURE

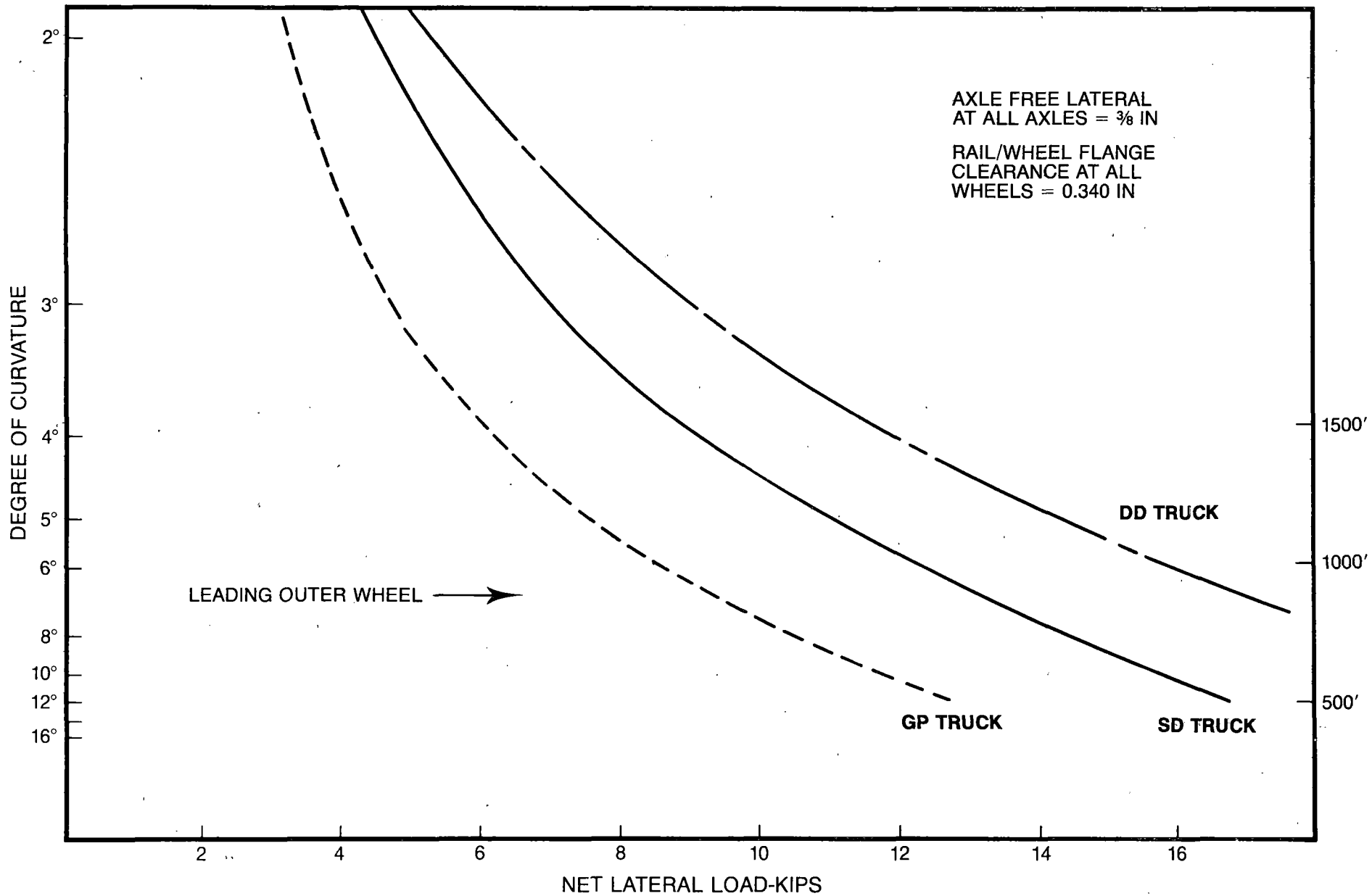

Figure 28
NET LATERAL LOAD v/s CURVATURE

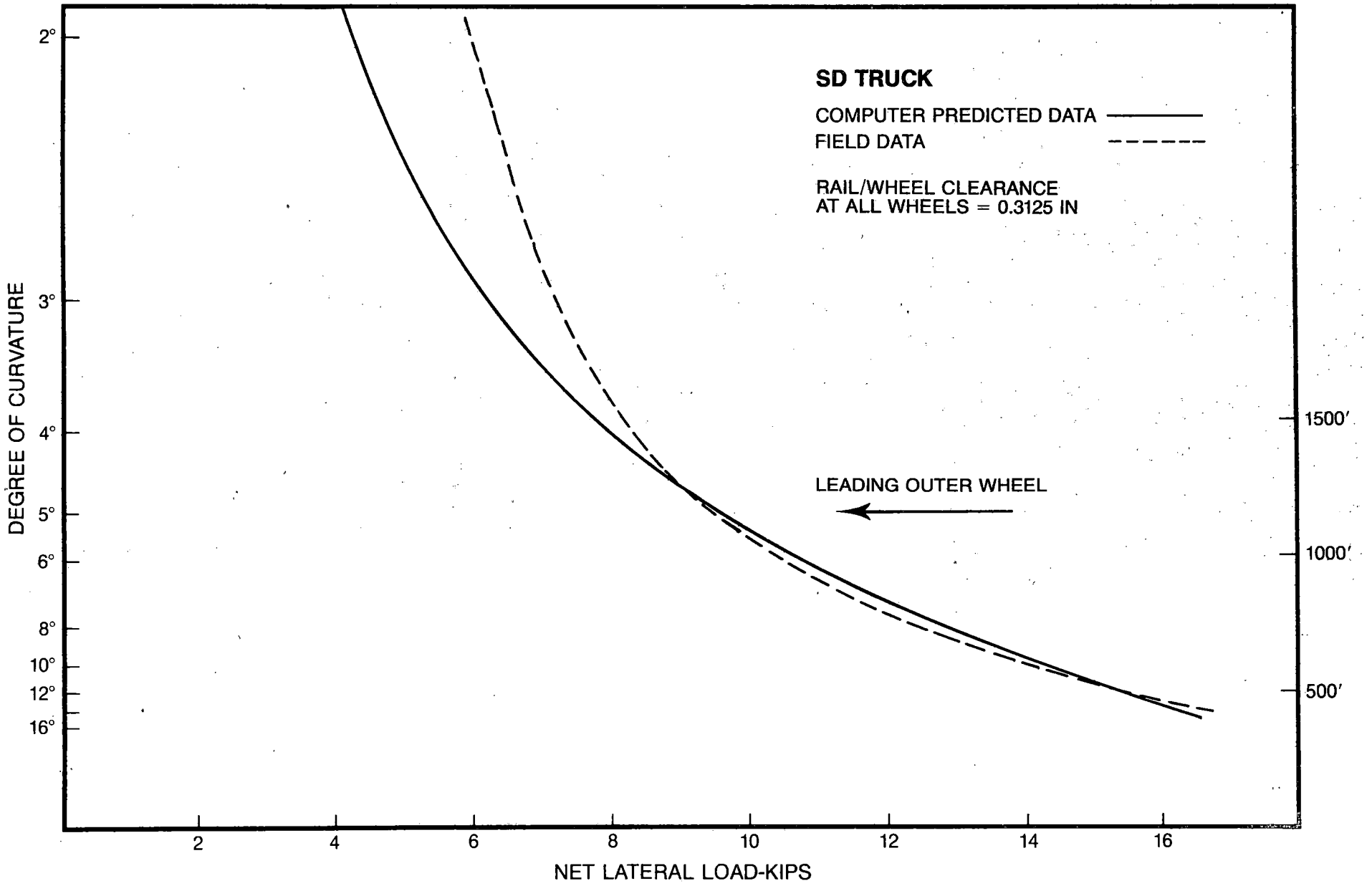

Figure 29
NET LATERAL LOAD v/s CURVATURE

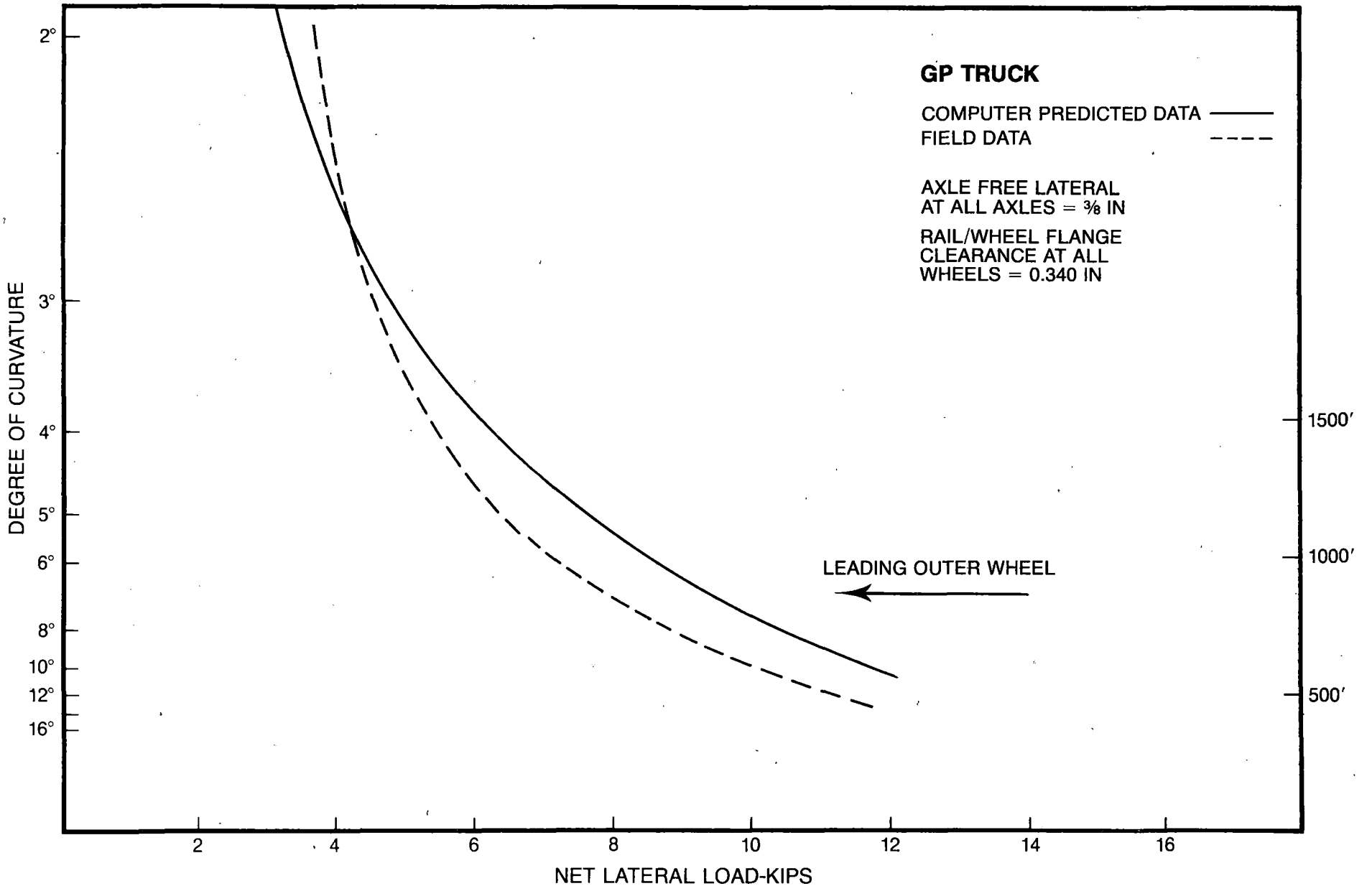

8. CONCLUSIONS

As mentioned at the outset in Section 7, the primary interest in curve negotiation is centered on the leading outer wheel, its guiding force and what can be done in the way of operating and design practices to control the magnitude of the net lateral load developed. For trucks with three or more axles, the importance of an intermediate axle in an externally guided mode has proven to be the most singly beneficial method of reducing the guiding force at the leading wheel. The intermediate axle can be made to play more of a role in many ways, increasing the free lateral, making the rubber donut less stiff, etc.; however, for a 2-axle truck there is very little that can be done. It should go without saying, that the shorter the wheelbase the better, refer to Figure 27.

One of the more detrimental practices to curve negotiation is the use of gauge widening on a curve where the truck is normally in first degree constraint. The additional clearance allows the truck to skew to a greater extent resulting in increased curving forces. Gauge widening does, however, have its merit, but only on sharper curves where second and final constraint may exist.

As a final point, the importance must be stressed of using an accurate friction-creep relationship in the modeling of a particular situation as the relationship changes greatly from coasting curving to curving with tractive effort to oily rail.

APPENDIX "A" - DERIVATION OF SINE AND COSINE SUBSTITUTIONS

Refer to the diagram in Figure 8 for the geometrical relationships being considered.

It can be seen that:

$$\cos\sigma = Dl/(R+G) \tag{1}$$

$$\sin\alpha = X/(R+S) = Dl/(R+G) \tag{2}$$

Therefore:

$$X = (R+S)\left[Dl/(R+G)\right] \tag{3}$$

This misalignment angle α between the wheel and rail is assumed to be a small angle, so that $\tan\alpha \simeq \sin\alpha$.

$$\tan\alpha = t/(G-S) \tag{4}$$

Combining with equation (2):

$$t = (G-S) \cdot Dl/(R+G) \tag{5}$$

Also:

$$U = Dl - t$$

$$= Dl - (G-S) \cdot Dl/(R+G)$$

$$= Dl\left(1 - \frac{G-S}{R+G}\right) \tag{6}$$

Therefore, the $\sin\sigma$ may be determined:

$$\sin\sigma = \cos\alpha = X/U$$

$$= \frac{R+S}{R+G - G+S} \tag{7}$$

$$= 1$$

In actuality σ is not exactly 90 degrees, but very close to it as small wheel/rail and axle/truck frame clearances would enter into the denominator; however, they are fractions of inches and in comparison to the curve radius terms may be neglected due to their small influence.

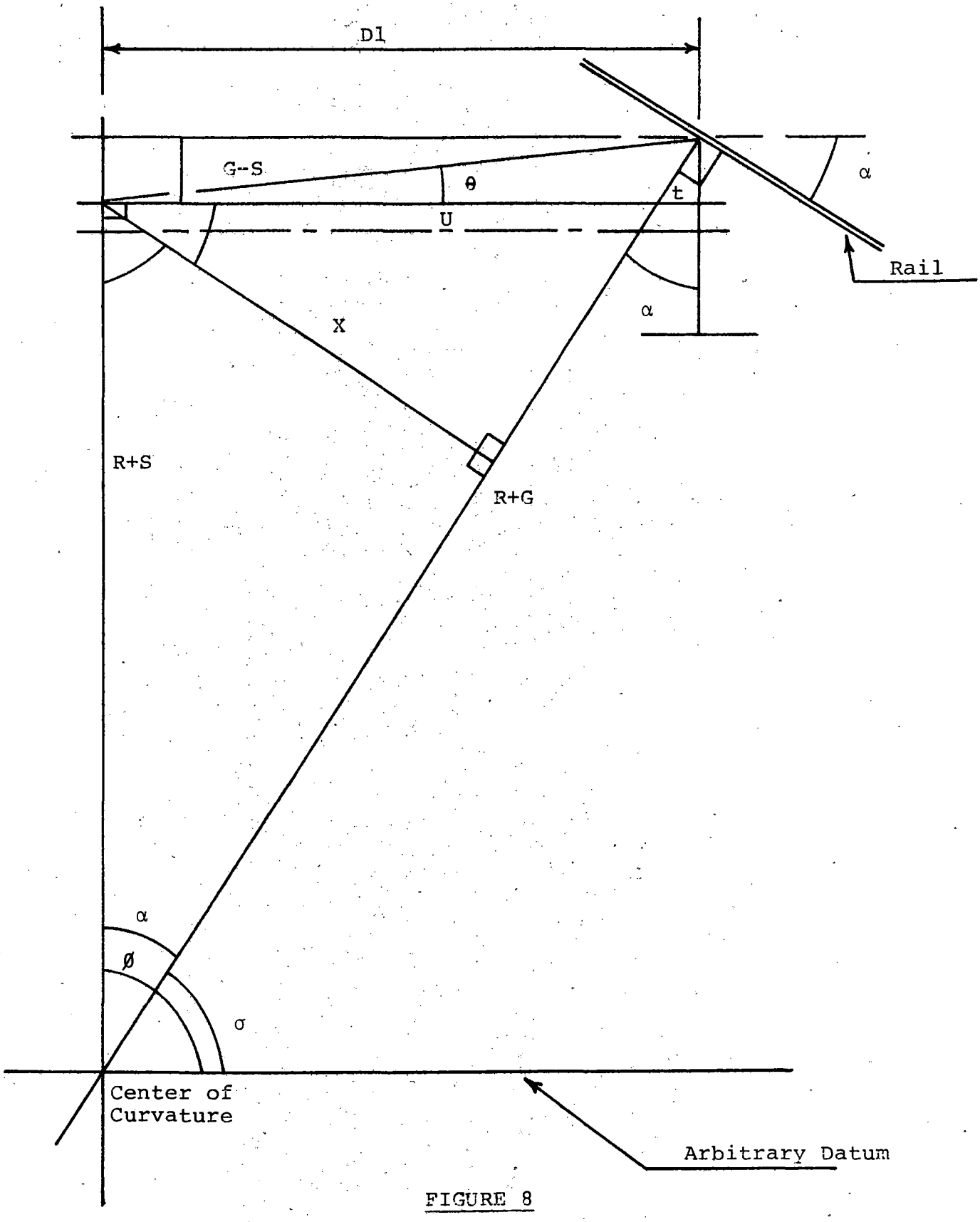
D1
G-S
θ
t
U
α
Rail
X
α
R+S
R+G
α
ø
σ
Center of
Curvature
Arbitrary Datum

FIGURE 8

With

$$\phi = \sigma + \alpha$$

$$\text{SIN } \phi = \text{SIN } \sigma \text{ COS} \alpha + \text{COS } \sigma \text{ SIN } \alpha$$

$$\text{SIN } \phi = 1 + (Dl/R+G)^2$$

The $(Dl/R+G)^2$ term may be considered very small, hence:

$$\text{SIN } \phi = 1 \qquad (8)$$

Solving then for COS ϕ:

$$\text{COS } \phi = \text{COS } \sigma \text{ COS } \alpha - \text{SIN } \sigma \text{ SIN } \alpha$$

$$= Dl/(R+G) - Dl/(R+G)$$

Therefore:

$$\text{COS } \phi = 0$$

APPENDIX "B" - CREEP AT INNER WHEELS

In the derivations of the equations to follow, refer to Figures 9 and 10. The derivation of the creep formulations at the inner or low rail side of the wheelset follows much the same procedure as that for the outer wheels outlined in Section 2.2 and 2.3. Initially, (refer to Figure 9) the inner wheel contact point on the rail may be defined with respect to the center of curvature as the track as:

Contact point on the wheel, W, in the X-direction:

$$W_X = (R+S)\ \text{COS}\ \phi + (D1^2 + (G+S)^2)^{1/2}\ \text{COS}\ \theta \qquad (1)$$

And in the Y-direction:

$$W_y = (R+S)\ \text{SIN}\ \phi - (D1^2 + (G+S)^2)^{1/2}\ \text{SIN}\ \theta \qquad (2)$$

(As long as the datum was chosen parallel to the truck centerline.)

The mating contact point on the rail, WR, may also be located with respect to the center of curvature in both the X and Y direction by:

$$WR_X = (R-G)\ \text{COS}\ \sigma \qquad (3)$$

$$WR_Y = (R-G)\ \text{SIN}\ \sigma \qquad (4)$$

The X and Y velocity components of the wheel and rail contact points, W and WR, respectively, may be found by differentiation of equations 1-4 with respect to time:

$$dW_X = V_{WX} = -(R+S)\text{SIN}\ \phi\ \dot{\phi} - (D1^2 + (G+S)^2)\ \text{SIN}\ \theta\ \dot{\theta} \qquad (5)$$

Similarly, , for the wheel in the Y-direction:

$$dW_y = (R+S)\ \text{COS}\ \phi\ \dot{\phi} - (D1^2 + (G+S)^2)^{1/2}\ \text{COS}\ \theta\ \dot{\theta} \qquad (6)$$

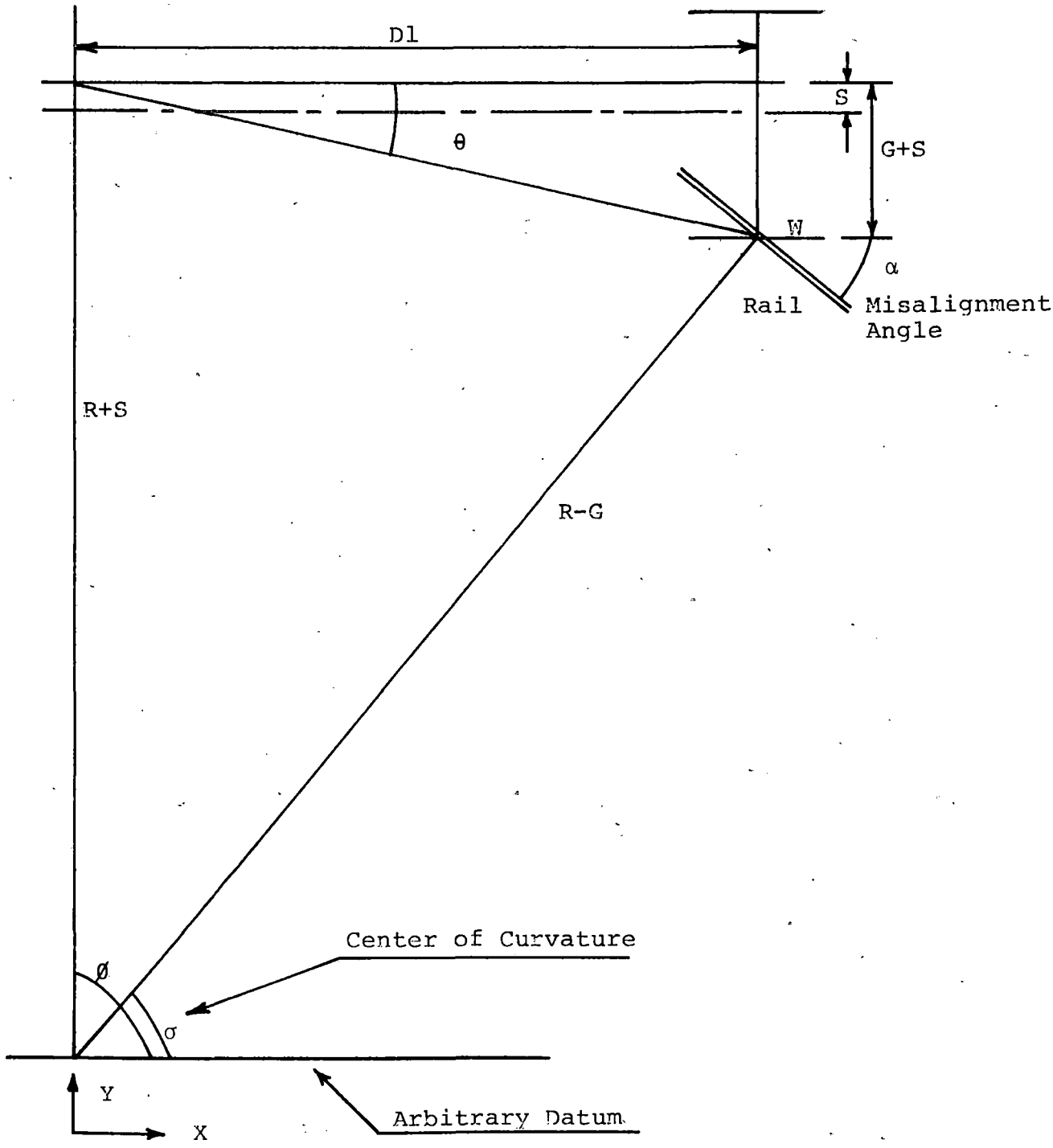
Dl
S
G+S
θ
W
α
Rail
Misalignment
Angle
R+S
R-G
Center of Curvature
ø
σ
Y
X
Arbitrary Datum

FIGURE 9

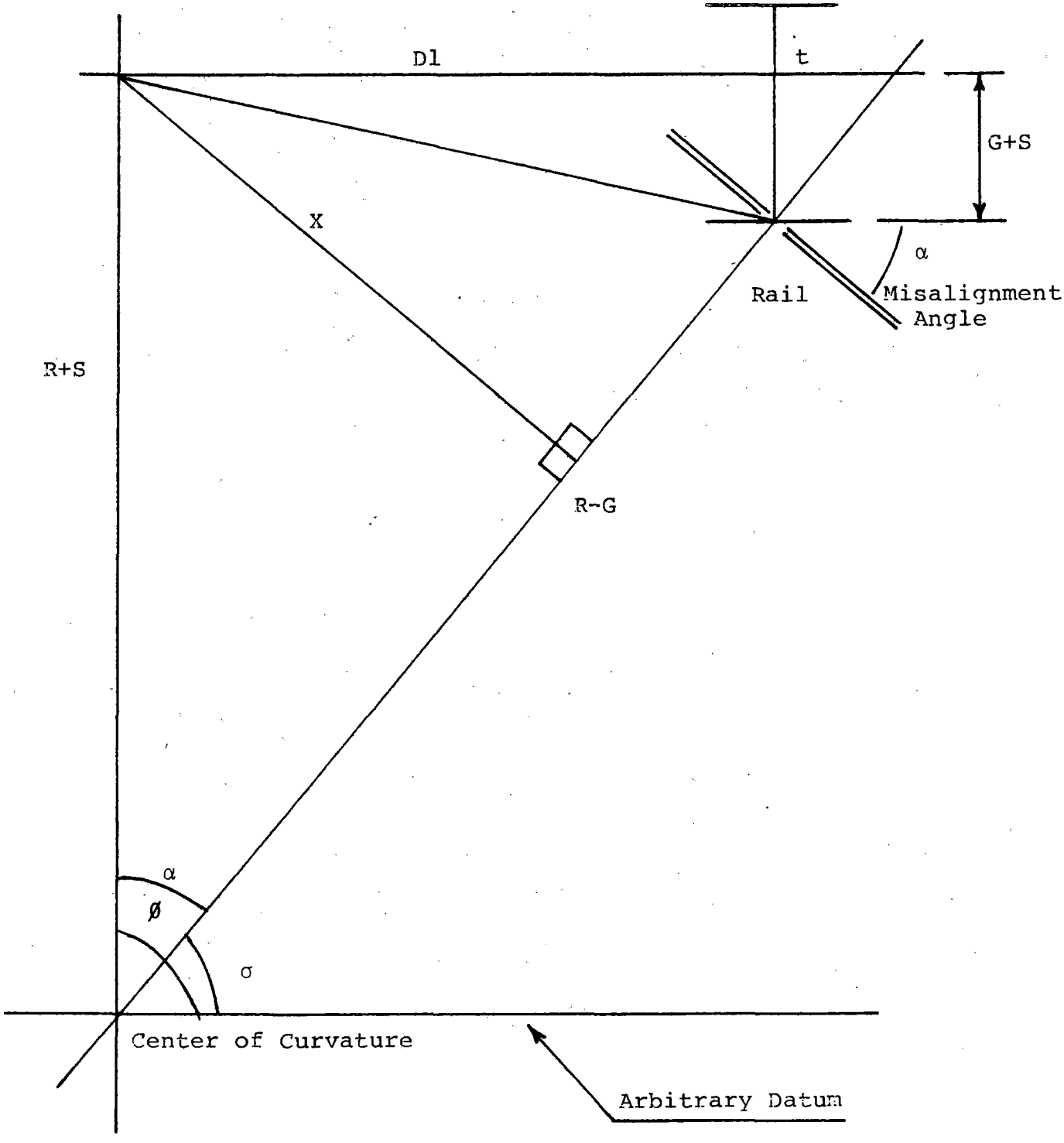
Dl
t
G+S
X
α
Rail
Misalignment
Angle
R+S
R-G
α
ø
σ
Center of Curvature
Arbitrary Datum

FIGURE 10

The velocity components of the rail contact point may be found as:

$$V_{wrx} = -\dot{\sigma}(R-G) \quad \text{SIN } \sigma \tag{7}$$

$$V_{wry} = \dot{\sigma}(R-G) \quad \text{COS } \sigma \tag{8}$$

In Section 2.2 it was shown that:

$$V = (R+S)\,\dot{\phi} \tag{9}$$

And:

$$\dot{\phi} = \dot{\sigma} \tag{10}$$

The slip velocity will be the difference in the rail and wheel contact point velocities. Therefore, the lateral slip velocity (Y-direction) may be written as:

$$\begin{aligned} S_{LAT} &= V_{wry} - V_{wy} \\ &= \dot{\phi}\left[(R-G)\ \text{COS}\,\sigma - (R+S)\ \text{COS}\ \phi\right] + \\ &\quad \dot{\theta}\ (D1^2 + (G+S)^2)^{\frac{1}{2}}\ \text{COS}\ \theta \end{aligned} \tag{11}$$

From Figure 9 COS θ may be found and inserted into (11) to yield:

$$\text{COS}\ \theta = D1/(D1^2 + (G+S)^2)^{1/2}$$

$$S_{LAT} = \dot{\phi}\{(R-G)\ \text{COS}\,\sigma - (R+S)\ \text{COS}\ \phi\} - D1\,\dot{\theta} \tag{12}$$

The longitudinal slip will become:

$$S_{LONG} = V_{wrx} - V_{wx}$$

$$S_{LONG} = \dot{\phi}\{(R+S)\ \text{SIN}\ \phi - (R-G)\ \text{SIN}\sigma\} + (G+S)\,\dot{\theta} \tag{13}$$

In order to furhter evaluate equations (12) - (13) the SIN, COS terms must be determined. This can be done by reference to Figure 10, and the use of the small angle assumption in dealing with the wheel/rail misalignment angle, or angle of attack. First, it may be observed that:

$$\cos\sigma = D1/(R-G) \tag{14}$$

$$\sin\alpha = X/(R+S) = D1/(R-G) \tag{15}$$

With the small angle assumption

$$\tan\alpha = t/(G+S) \tag{16}$$

$$\simeq D1/(R-G) \tag{17}$$

Combination of equations (16) and (17) yields:

$$t = D1\ (R+S)/(R-G) \tag{18}$$

Next define:

$$U = D1 + t \tag{19}$$

$$= D1\{1 + (G+S)/(R-G)\}$$

With this $\sin\sigma$ may be determined:

$$\sin\sigma = \cos\alpha = X/U$$

$$= \frac{(R+S)\ D1}{R-G} \cdot \frac{1}{D1\ (1 + \frac{G+S}{R-G})}$$

$$\sin\sigma = \frac{R+S}{R-G + G+S} \tag{20}$$

Therefore, $\sin\sigma$ may be considered as 1. With $\phi = \sigma + \alpha$ the $\sin\phi$ can be found as:

$$\sin\phi = \sin\sigma\cos\alpha + \cos\sigma\sin\alpha$$

Or upon reduction:

$$\sin\phi = 1 + (D1/R-G)^2 \tag{21}$$

With the radius R in the denominator the $(D1/R-G)^2$ term in equation (21) may be considered small, making:

$$\sin\phi = 1 \tag{22}$$

Hence:

$$\cos\phi = 0 \tag{23}$$

Insertion of equations (14), (20), (22), and (23) into the slip velocity equations, (12) and (13) gives the simplified versions of:

$$S_{LAT} = Dl \ (\dot{\phi} - \dot{\theta}) \tag{24}$$

$$S_{LONG} = (G+S) \ (\dot{\phi} + \dot{\theta}) \tag{25}$$

Again, recalling that for steady state curving $\theta = 0$, or there is a constant truck rotation with respect to the track for a constant radius of curvature. The slip equations reduce to:

$$S_{LAT} = \dot{\phi} \cdot Dl$$

$$S_{LONG} = \dot{\phi} \cdot (G+S)$$

Now the angular velocity term, $\dot{\phi}$, may be replaced by equation (9) or:

$$S_{LAT} = V \cdot Dl/(R+S) \tag{26}$$

$$S_{LONG} = V \cdot (S+G)/(R+S) \tag{27}$$

With the creep defined as the slip velocity divided by the roll velocity, the lateral and longitudinal creep components may now be found as:

$$\text{LATERAL CREEP} = S_{LAT}/V = Dl/(R+S) \tag{28}$$

$$\text{LONGITUDINAL CREEP} = S_{LONG}/V = (S+G)/(R+S) \tag{29}$$

Combining equations (28) and (29) to solve for the magnitude of the resultant creep on an inner wheel we get:

$$\text{CREEP} = (Dl^2 + (S+G)^2)^{1/2} \cdot \{1/(R+S)\} \tag{30}$$

APPENDIX C - CENTERPLATE BREAKAWAY MOMENT & RADIUS DIFFERENTIAL CREEP

1. CENTERPLATE BREAKAWAY MOMENT

The model has an optional input to simulate the moment that resists (initially only) the rotation of the truck as it enters a curve. The moment is analogous to that encountered when opening a jar; once overcome, the rotation is unrestricted.

2. RADIUS DIFFERENTIAL CREEP

Additional creep may be introduced due to the slip velocity existing when wheel radii on a truck differ. If V_T is the longitudinal truck speed, R_{AVG} is the average wheel radius of the truck and $\dot{\Omega}_{AVG}$ is the average radial velocity at the wheel rail interface,

$$\text{If } V_T = R_{AVG}\,\dot{\Omega}_{AVG}$$

Letting V_{SN} represent the slip velocity due to the radius differential and R_N the radius at the wheel under consideration,

$$V_{SN} = R_{AVG}\,\dot{\Omega}_{AVG} - R_N\,\dot{\Omega}_{AVG}$$

$$V_{SN} = (R_{AVG} - R_N)\,\dot{\Omega}_{AVG}$$

The creep at wheel N is therefore

$$\text{CREEP}_N = \frac{R_{AVG} - R_N\,\dot{\Omega}_{AVG}}{V_T} \qquad \text{(longitudinal)}$$

This creep is incorporated into the equations as creep at inner rail (negative) and outer rail (positive). The ultimate sign is dependent on whether the radius at the wheel specified is larger or smaller than the average. In the equations below, CI and CØ represent this creep factor normalized to be dimensionally consistent, i.e.,

$$CI = CREEP_{N(INSIDE)} \cdot (R+S)$$

$$C\emptyset = CREEP_{N(OUTSIDE)} \cdot (R+S)$$

The modified equations (28 and 29) for resultant creep are then,

$$A_o = (D1^2 + (S-G+C\emptyset)^2)^{\frac{1}{2}}/(R+S) \qquad (28A)$$

$$A_i = (D1^2 + (S+G-CI)^2)^{\frac{1}{2}}/(R+S) \qquad (29A)$$

APPENDIX D - LIST OF FIGURES

REFERENCES

1. Marta, H. A., and Mels, K. D., "Wheel-Rail Adhesion", ASME Paper No. 68-WA/RR-1.

2. Eksergian, R., "Static Adjustment of Trucks on Curves", ASME Transactions, Vol. 42, No. 1776, 1920.

3. Wickens, A. H., "General Aspects of the Lateral Dynamics of Railway Vehicles", ASME Paper No. 68-WA/RR-3.

4. Johnson, K. L., "The Effect of Spin Upon the Rolling Motion of an Elastic Sphere on a Plane", Journal of Applied Mechanics, September, 1958.

5. Marta, H. A., Mels, K. D., and Itami, G. S., "The Friction Creep Phenomenon of Adhesion Between Steel Wheels and Rails".

6. Newland, D. E., "Steering a Flexible Railway Truck on Curved Track", ASME Paper No. 69-RR-5.

7. Koffman, J. L., "Negotiation of Curves by Vehicles", Rail Engineering International, July 1972.

8. Koci, L. F., and Marta, H. A., "Lateral Loading Between Locomotive Truck Wheels and Rail Due to Curve Negotiation", ASME Paper No. 65-WA/RR-4.

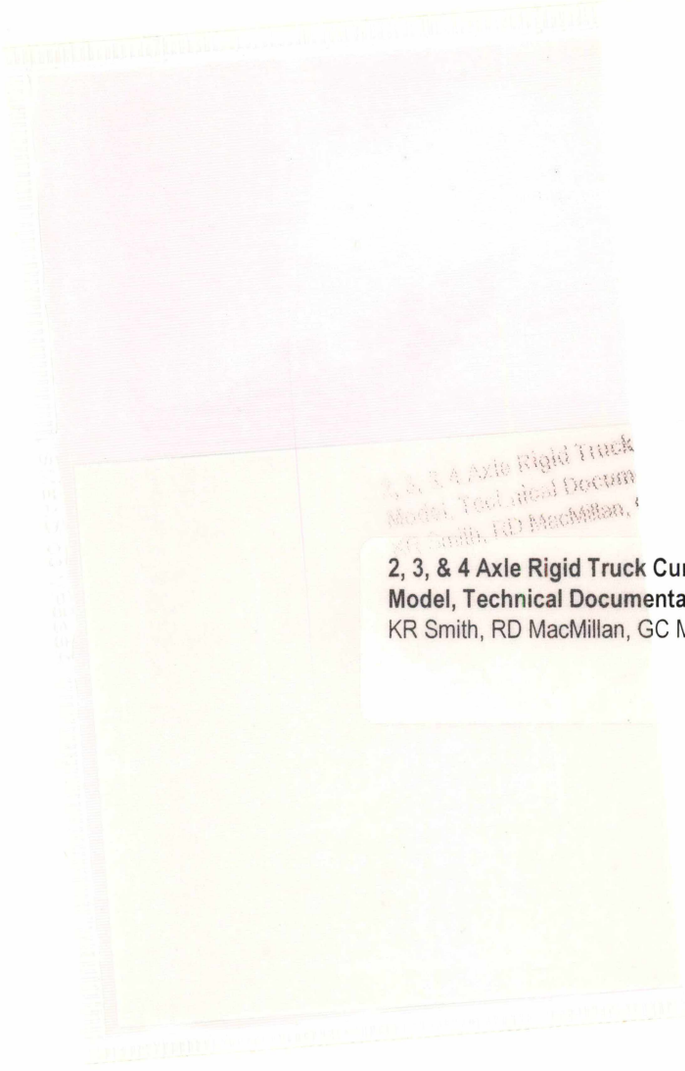

2, 3, & 4 Axle Rigid Truck Curve Negotiation Model, Technical Documentation,
KR Smith, RD MacMillan, GC Martin